STELLAR TURBULENT CONVECTION: A NEW MODEL AND APPLICATIONS

V. M. CANUTO

NASA/Goddard Space Flight Center, Institute for Space Studies, 2880 Broadway, New York, NY 10025

AND

I. MAZZITELLI

Istituto di Astrofisica Spaziale, CNR, CP 67, 00044 Frascati, Italy

ABSTRACT

In the interior of stars, convective turbulence (1) is characterized by eddies of all sizes and (2) is compressible (the sound speed is finite). The mixing-length theory (MLT) approximates the first by assuming that there is only one large eddy, and the second by treating turbulence as incompressible.

Here, we correct the first MLT approximation. Using two modern theories of turbulence, we compute the full spectrum of eddies and propose a new formula for the turbulent convective flux F_c to replace the corresponding MLT expression. At high convective efficiencies, *the new F_c is up to 10 times larger than F_c(MLT)*, a result recently confirmed by direct numerical simulation of turbulent convection. We also calculate the turbulent pressure exactly.

As for the second MLT approximation, we retain the incompressibility condition but improve over the MLT by employing two expressions for the mixing length: (1) the standard $\Lambda = \alpha H_p$ and (2) a new expression free of adjustable parameters, $\Lambda = z$, where z is the distance to the top of the convective zone.

We apply the new model to study the evolution of a $1\,M_\odot$ star and of a globular cluster star of $0.8\,M_\odot$. With $\Lambda = \alpha H_p$, the fit to the data requires $\alpha = 0.7$, thus eliminating the inconsistency of an $\alpha > 1$ usually required by the MLT formalism.

With $\Lambda = z$, we fit the effective temperature of the Sun within 0.2% without free parameters. Implications for helioseismology are briefly discussed. We also discuss the evolutionary tracks of a solar red giant, a globular cluster main sequence, and a red giant of $0.8\,M_\odot$. The new model predicts a subatmospheric density inversion larger than that given by the MLT. Also, the observational turnoff of globular clusters requires a larger mass and thus a younger age, a result of possible cosmological interest. Future applications of the new model are discussed, together with suggestions of how to incorporate the new model in stellar evolutionary codes.

Although much work remains to be done to assess the compatibility of the new model with a wider set of observational data, as well as to treat compressibility effects, we believe that the three new ingredients, (1) *the full spectrum of turbulent eddies*, (2) *the absence of free parameters in the $\Lambda = z$ model*, and (3) *the fit to the Sun's data*, have resulted in a model considerably more robust and complete than the MLT.

Subject headings: convection — stars: interiors — turbulence

1. INTRODUCTION

Meaningful comparisons between the theory of stellar evolution and observational data became possible after Biermann (1948), Vitense (1953), and Böhm-Vitense (1958) proposed the adoption of the mixing-length theory (MLT) to treat turbulent convection in stars. The MLT has a long history. Originally proposed a century ago, it was greatly expanded by the schools of fluid dynamicists led by Prandtl (1925) and von Kármán (1930), who used it to describe engineering turbulent flows, e.g., channel flow, pipe flow, etc. The results were surprisingly good, considering that a phenomenon as complex as turbulence was described by a relatively simple model that contained essentially one adjustable parameter, the mixing length. Undoubtedly, the simplicity and success of the MLT played a considerable role in the suggestion that it be applied to describe stellar interiors.

While the MLT has proved to be a useful tool in astrophysics, it remains an incomplete model with many unsolved problems that repeated attempts over the years have been unable to resolve satisfactorily (for recent work see Pederson, VandenBerg, & Irwin 1990; Spruit, Nordlund, & Title 1990;

Massaguer 1990). In this paper we attempt to resolve two main limitations of the MLT:

1. *The MLT treats the energy spectrum of the turbulent eddies as if it consisted of only one large eddy.*—To correct for this assumption, we begin by inquiring under what approximation a general model of convective turbulence yields the MLT expressions. First, in § 2.4, we use an analytical approach and show that *if* the turbulence energy spectrum is assumed to be a delta function (which implies only one eddy), one recovers the MLT expression for the convective flux. Second, when we solve the full model of turbulence for arbitrary values of the viscosity, we show that in a viscous flow the number of eddies contributing to the convective flux is small (Figs. 1–3); conversely, for a nearly inviscid system, such as the interior of a star, the number of eddies contributing to the flux is very large. *We thus conclude that the one-eddy model adopted by the MLT may be considered a reasonable approximation for viscous flows, but is a poor approximation for nearly inviscid stellar interiors which are characterized by a wide spectrum of eddies of all sizes.*

In this paper we employ two modern theories of turbulence to derive the full spectrum of turbulent eddies (the ratio of the

largest to the smallest is greater than 10^6) which, in turn, we use to evaluate the new expression for the convective flux.

2. *The MLT does not provide the mixing length* Λ.—In § 2.8 we discuss the fact that under the conditions of incompressibility ($c_s^2 \to \infty$) and high convective efficiency, the equations describing the turbulent flow do not provide a natural unit of length. The assumption that turbulence is incompressible is usually made because it provides a considerable mathematical simplification, although it is physically incorrect in stellar interiors. To balance mathematical tractability without sacrificing a main physical feature, one employs a hybrid approach: turbulence is treated as incompressible, but Λ is written as $\Lambda = \alpha H_p$, i.e., one tries to accommodate the fact that convective eddies should be smallest near the top and become larger with increasing depth (for the phenomenon of vertical stacking of eddies see § 2.8).

The compromise succeeds only at the expense of having to introduce the adjustable parameter α, which ultimately undermines the ability of theoretical models to make predictions and which, from the point of view of stellar modeling, has been a major source of discomfort. Specifically, within the MLT the value of α is usually fixed (Mazzitelli 1979) by requiring that 1 $M_\odot$ with $Z = 0.02$ has the observed $T_{\rm eff}$ at an age of 4.7 Gyr. This requires $1.4 \le \alpha \le 1.6$ and $0.26 < Y < 0.28$ (VandenBerg & Bell 1985; Maeder & Meynet 1989). Several criticisms can be raised against this tuning of α. For example, there is no *a priori* reason why the conditions in the solar subatmosphere should also exist in red giants or/and white dwarfs, where the physical parameters are orders of magnitude different. Also, there is no reason why the same α should apply to the entire convective zone: in fact, helioseismological data seem to indicate that the MLT does not provide a satisfactory description of the surface regions (Dziemboski, Paternò, & Ventura 1988); last, a value of $\alpha > 1$ may be considered inconsistent with the MLT, since in most cases the thickness of the overadiabatic region is only a fraction of H_p.

Since we are not yet in a position to treat compressible turbulence (except with numerical simulations; see § 2.8), we account for it via the mixing length and of course via the adiabatic gradient. However, when we adopt the expression $\Lambda = \alpha H_p$, our model requires $\alpha < 1$, which is a more consistent value. Furthermore, in § 2.8 we present physical arguments borrowed from atmospheric turbulence to suggest a new expression for Λ with no adjustable parameters, namely, $\Lambda = z$, where z is the distance from any point in the convective zone (CZ) to the top of it.

The new model, equations (3) and (32), yields a convective flux up to an order of magnitude larger than the MLT value (see Fig. 5). It is important to stress that this result has been recently confirmed by a direct numerical simulation of turbulent convection (Cabot et al. 1990) and that it is in accord with the results of Chan & Sofia (1989), who found that the MLT underestimates F_c.

The new model, together with the two expressions for Λ discussed above, is then applied to study two evolutionary cases of interest, the Sun and a globular cluster star of 0.8 $M_\odot$. First, using $\Lambda = \alpha H_p$, we obtain a good fit to the Sun with $\alpha = 0.7$. With $\Lambda = z$, and thus no adjustable parameters, we fit the Sun within 0.2% (Figs. 6 and 7). By contrast, with $A = z$, the MLT fails to achieve this goal (Fig. 7, *curve* 4). The new temperature profile of the more external subatmospheric solar layers is steeper than in the MLT case. This leads to larger values of the speed of sound, a welcome feature to helio-

seismological studies. Both for the Sun and for a globular cluster star, $T_{\rm eff}$ at the turnoff is lower than in the MLT case, as is the difference in $T_{\rm eff}$ between turnoff and the base of the red giant branch. These features require larger turnoff masses to fit the observed H-R diagrams for open and globular clusters, thus implying lower ages, which is a result with possible cosmological implications. Since the new convective fluxes are larger than the MLT values, the velocities of the convective elements are correspondingly lower than previously assumed, which may be relevant when considering overshooting. The larger fluxes may also imply a different behavior for the second and third dredge-up in advanced evolutionary phases.

Although the new model with $\Lambda = z$ is nonlocal, we show how it can be easily implemented in existing evolutionary codes (§ 3.1).

2. THEORY

2.1. *The New Model versus the MLT*

Assuming that the depth of the convective layer is small compared with the radius of the star, we define a locally Cartesian coordinate system in which the z-axis is directed radially outward. The turbulent convective flux F_c is then given by

$$F_c = c_p \rho \langle w\theta \rangle , \qquad (1)$$

where w is the z-component of the turbulent velocity v, and θ is the fluctuating component of the temperature. Equation (1) may be more conveniently written as

$$F_c = -K_t \left[\frac{dT}{dz} - \left(\frac{dT}{dz} \right)_{\rm ad} \right], \qquad (2)$$

or, equivalently, as (H_p is the pressure scale height)

$$F_c = KTH_p^{-1}(\nabla - \nabla_{\rm ad})\Phi(\nabla - \nabla_{\rm ad}, A) , \qquad (3)$$

where $K = 4acT^3/3\kappa\rho$ is the radiative conductivity, while K_t is the turbulent thermal conductivity. The dimensionless function $\Phi = K_t/K$ is in general a function of $\nabla - \nabla_{\rm ad}$ and of the thermodynamic quantities represented by the parameter A. In terms of the Nusselt number N, $N = \Phi + 1$.

Different models of turbulence yield different functions Φ. For example, the MLT expression for Φ is ($a_0 = 9/4$) (Gough & Weiss 1976; Cox & Giuli 1968, hereafter CG68).

$$\Phi^{\rm MLT} = \tfrac{1}{2} a_0 \Sigma^{-1}[(1 + \Sigma)^{1/2} - 1]^3 , \qquad (4)$$

$$\Sigma \equiv 4A^2(\nabla - \nabla_{\rm ad}) , \qquad (5)$$

$$A = \frac{c_p \rho^2 \kappa \Lambda^2}{12acT^3} \left(\frac{g}{2H_p} \right)^{1/2} = \frac{\Lambda^2}{9\chi} \left(\frac{g}{2H_p} \right)^{1/2} , \qquad (6)$$

where Λ is the mixing length and $\chi = K/c_p\rho$ is the thermometric conductivity.

The goal of this paper is to provide a new expression for Φ, *equation (32), to replace the* MLT *expression equation (4).*

As we shall see, the natural variable entering the new convective model is not Σ but

$$S = \sigma \, {\rm Ra} = (81/2)\Sigma . \qquad (7)$$

where $\sigma = \nu/\chi$ is the Prandtl number and Ra is the Rayleigh number (Ra $= g\alpha\beta\Lambda^4/\nu\chi$; for α and β see eq. [14]). Furthermore, if one introduces the convective efficiency Γ,

$$2\Gamma + 1 = (1 + \Sigma)^{1/2} , \qquad (8)$$

the total flux (convective plus radiative) $F_{\rm total} = F_c + F_{\rm rad}$, with

$F_{\text{total}} = KTH_p^{-1}\nabla_r$ and $F_{\text{rad}} = KTH_p^{-1}\nabla$, yields an equation for Γ in terms of known quantities. In the MLT case, the result is the well-known cubic equation

$$a_0 \Gamma^3 + \Gamma^2 + \Gamma - \delta = 0 , \qquad (9)$$

$$\delta \equiv A^2(\nabla_r - \nabla_{\text{ad}}) . \qquad (10)$$

In the new model, equation (9) will be replaced by equation (36).

Equations (2)–(6) coincide with equation (14.108) of CG68; equation (8) coincides with equation (14.106) of CG68; and equations (9) and (10) coincide with equation (14.82) of CG68.

2.2. *The Expression for F_c*

The description of heat transfer by turbulent rather than laminar convection is a difficult problem primarily because turbulence is a highly nonlinear, diffusive phenomenon. A physical property such as kinetic energy is shared among a large number of *eddies*, the sizes of which range from almost molecular to the dimensions of the system itself. A main challenge of a turbulence theory is to determine the distribution of turbulent kinetic energy among the various eddies. The key quantity is the turbulent energy spectrum function $E(k)$, defined so that the turbulent kinetic energy per unit mass is (Batchelor 1953)

$$\tfrac{1}{2}v_t^2 = \int_0^\infty E(k)dk . \qquad (11)$$

Since the scale size ℓ of an eddy can be related to k by $\ell = \pi/k$, the integration over k is in a sense equivalent to the integration over all eddy sizes.

The convective flux F_c given by equation (1) can be expressed in terms of $E(k)$ by (see, e.g., Yamaguchi 1963)

$$F_c = \frac{c_p \rho}{g\alpha} \int_0^\infty 2E(k)[n_s(k) + \nu k^2]dk , \qquad (12)$$

so that, when F_c is cast in the general form (3), the expression for the dimensionless function Φ becomes

$$\Phi = \frac{1}{g\alpha\beta\chi} \int_0^\infty 2E(k)[n_s(k) + \nu k^2]dk , \qquad (13)$$

where

$$\alpha = T^{-1}, \quad \beta = T(\nabla - \nabla_{\text{ad}})H_p^{-1} . \qquad (14)$$

Here α is the thermal expansion coefficient, β is the superadiabatic temperature gradient, and ν is the kinematic viscosity.

The function $n_s(k)$ represents the rate at which energy is injected into the system to keep the turbulence from decaying. In this paper, n_s is regarded as a known quantity, equation (18). For the generalization of equations (12) and (13) to include magnetic fields and rotation, as well as a derivation of equation (12) itself, see Canuto & Hartke (1986).

2.3. *The Non-linear Equation for the Turbulence Energy Spectrum Function $E(k)$*

As equations (1), (12), and (13) indicate, the evaluation of the convective flux requires w and θ, which satisfy the coupled Navier-Stokes and temperature equations that describe turbu-

lent convection (Chandrasekhar 1961)

$$\frac{\partial v(x, t)}{\partial t} + v(x, t) \cdot \nabla v(x, t)$$
$$= -\nabla p(x, t) + \nu\nabla^2 v(x, t) + g\alpha\theta(x, t)\lambda , \qquad (15a)$$

$$\frac{\partial \theta(x, t)}{\partial t} + v(x, t) \cdot \nabla\theta(x, t) = \chi\nabla^2\theta(x, t) + \beta w\lambda , \qquad (15b)$$

where p is the pressure divided by the constant density and $\lambda = (0, 0, 1)$.

The difficulty in solving equations (15) is due to the nonlinear terms in both equations. Fourier expansion of $v(x, t)$ and $\theta(x, t)$ in normal modes yields the equations satisfied by each Fourier amplitude $v_i(k, t)$ and $\theta(k, t)$:

$$\left[\frac{\partial}{\partial t} - n_s(k)\right]v_i(k, t)$$
$$+ \frac{1}{2}i\Pi_{ijm}\iint d^3q\, d^3p\, \delta^3(k - p - q)v_j(q, t)v_m(p, t) = 0 , \qquad (16a)$$

$$\left[\frac{\partial}{\partial t} - n_s(k)\right]\theta(k, t)$$
$$+ ik_j \iint d^3q\, d^3p\, \delta^3(k - p - q)v_j(k, t)\theta(p, t) = 0 , \qquad (16b)$$

where $\delta^3(x)$ is the three-dimensional Dirac delta function and Π_{ijm} is defined as ($T_{ij} = \delta_{ij} - k_i k_j/k^2$, where δ_{ij} is the Kronecker delta symbol) $\Pi_{ijm} = k_j T_{im} + k_m T_{ij}$.

The rate n_s originates from the fact that in going from equation (15) to equation (16) one takes

$$\beta w(k) = (n_s + \chi k^2)\theta(k) ,$$

$$g\alpha\theta(k)\frac{x}{1 + x} = (n_s + \nu k^2)w(k) , \qquad (17)$$

which yields the expression for $n_s(k)$ (Rayleigh 1916; Chandrasekhar 1961)

$$2n_s(k) = -(\nu + \chi)k^2 + [(\nu - \chi)^2k^4 + 4g\alpha\beta x(1 + x)^{-1}]^{1/2} , \qquad (18)$$

where x accounts for the possible anisotropy in the eddy sizes, $x = (k_x^2 + k_y^2)/k_z^2$.

Given n_s, the nonlinear equations (16) provide the amplitudes $v_i(k, t)$, which in turn yield the energy spectrum $E(k)$ defined as

$$E(k, t) = 4\pi k^2 \langle v_i^*(k, t)v_i(k, t)\rangle . \qquad (19)$$

Substitution of equations (18) and (19) in equation (13) would yield the convective flux.

Unfortunately, equations (16) cannot be solved exactly. Nevertheless, the last two decades have witnessed great progress in devising approximation schemes that allow the computation of $E(k)$. The best models presently available are the DIA model (Direct Interaction Approximation; Kraichnan 1964; Leslie 1973), the EDQNM model (Eddy Damped Quasi-Normal Markovian; Orszag 1977, Lesieur 1987), and the RNG model (Renormalization Group; Yakhot & Orszag 1986). For extensive reviews of both the theories and their applications, see Leslie (1973) and Lesieur (1987). An analytical model to treat the large portion of the eddy spectrum has also been proposed (Canuto & Goldman 1985).

Multiplying equation (16a) by $v_i^*(k, t)$, performing an ensemble average using equation (19), and treating the nonlinear terms following the rules of EDQNM (for details see Orszag 1977), the equation determining $E(k)$ becomes (for the case of DIA see Appendix A)

$$\left[\frac{\partial}{\partial t} - 2n_s(k)\right]E(k, t) = T(k, t) , \qquad (20)$$

where the nonlinear transfer $T(k, t)$ is given by

$$T(k, t) = \int_\Delta\!\!\int dp\, dq\, E(q)$$
$$\times [k^2 E(p) - p^2 E(k)]a(p, q, k)\theta(k, p, q) . \quad (21)$$

For brevity we have omitted the time dependence of E and θ in equation (21). Here $a(p, q, k) = (xy + z^3)/q$, where x, y, and z are the cosines of the angles opposite k, p, and q, and the symbol Δ signifies that the integration over p and q is such that $k = q + p$. The function $\theta(k, p, q)$ represents the correlation time scale governing the nonlinear interactions, and, given the large variety of eddy sizes, θ depends rather sensitively on which group of eddies is considered, since large eddies exist longer than small eddies. To complete equations (20) and (21), we must add the equations for θ (Kraichnan 1987), i.e.,

$$\frac{\partial\theta(k, t)}{\partial t} = 1 - 2n_c(k, t)\theta(k, t) ,$$

$$n_c(k, t) = k^2[v + v_t(k, t)] , \qquad (22)$$

$$v_t(k, t) = \tfrac{1}{15}\int_k^\infty \theta(p, t)[5E(p, t) + pE'(p, t)]dp .$$

Here, $v_t(k, t)$ is the turbulent viscosity, and $E'(p, t) \equiv dE(p, t)/dp$.

Equations (20)–(22) are the basic equations of turbulence that determine the turbulent energy spectrum $E(k)$. Among the many tests of equations (20)–(22), it has been shown that they yield the well-known Kolmogorov spectrum $E(k) \propto k^{-5/3}$, which has received the most experimental confirmation (Monin & Yaglom 1975; Lesieur 1987).

In this paper we shall solve equations (20)–(22) for the case of convection, derive the corresponding $E(k)$, evaluate F_c, and compare the result with that of the MLT (CG68; Gough & Weiss 1976; Langer 1986; Renzini 1987; Spruit et al. 1990). However, since the numerical solutions of equations (20)–(22) that we shall present are the result of complicated nonlinear processes among turbulent eddies that cannot be readily seen by inspecting equation (21), and in order to avoid the impression that equations (20)–(22) are a black box, we discuss the physics of $T(k)$ in Appendix B.

2.4. *The MLT as a Special Case of the General Theory: The Ensuing Inconsistencies*

Although the MLT is usually not formulated in the language of turbulence theory and therefore not expressed in terms of $E(k)$, we shall do so here. Consider the approximation

$$E(k) \to E^{MLT}(k) = E_0\,\delta(1 - k/k_0) , \qquad (23)$$

where $\delta(x)$ is a delta function peaked around some large eddy of wavenumber $k_0 \approx \Lambda^{-1}$. Inserting equation (23) in equations (20)–(22), and assuming stationarity, gives $E \sim n_s^2 k_0^{-3}$, which, substituted in equation (12), yields

$$F_c \sim \frac{c_p\rho}{g\alpha} n_s^3(k_0)k_0^{-2} . \qquad (24)$$

Next we use equation (18) with $k = k_0$ and zero viscosity. Using equation (3), the resulting Φ is

$$\Phi \approx S^{-1}[(1 + S)^{1/2} - 1]^3 , \qquad (25)$$

where $S = (81S_0/2)\Sigma$ and $S_0 = 4x\pi^{-4}(1 + x)^{-3}$, since we have taken $k_0\Lambda = \pi(1 + x)^{1/2}$. Within numerical factors (which cannot be fully determined unless one adopts a model for the eddy anisotropy factor x), equation (25) coincides with the MLT expression (4). We have therefore shown that when equation (23) is used in the full turbulence model, equations (20)–(22), the result is the MLT expression for F_c.

Next, we shall show that the MLT expression for $E(k)$, equation (23), describes the high-viscosity limit of the true $E(k)$, which we shall formally write as $E(k, v)$ to exhibit its dependence on v. In Figures 1–3 we show the dependence of $E(k, v)$ on the viscosity v. The largest eddies containing most of the energy are found in the region around k_0, whereas the region beyond k_d corresponds to the smallest eddies, where dissipation of energy by viscosity occurs. The value of k_d is determined by the value of v via (Landau & Lifshitz 1987)

$$k_d \propto v^{-3/4} , \qquad (26)$$

so that in a highly viscous system k_0 and k_d almost coincide, i.e., only large eddies are found. By contrast, in a low-viscosity system $k_d \gg k_0$ (Figs. 1–3), and one must consider a much wider range of eddy sizes. We thus have

$$\begin{aligned}v \to \infty: \quad & k_0 \approx k_d \quad \text{or} \quad \ell_0 \approx \ell_d \\ v \to 0: \quad & k_d \gg k_0 \quad \text{or} \quad \ell_0 \gg \ell_d .\end{aligned} \qquad (27)$$

Expressed in more quantitative terms, in a physical system of arbitrary viscosity v, the ratio ℓ_0/ℓ_d of the largest to the smallest eddy can be expressed, for the case of large convective
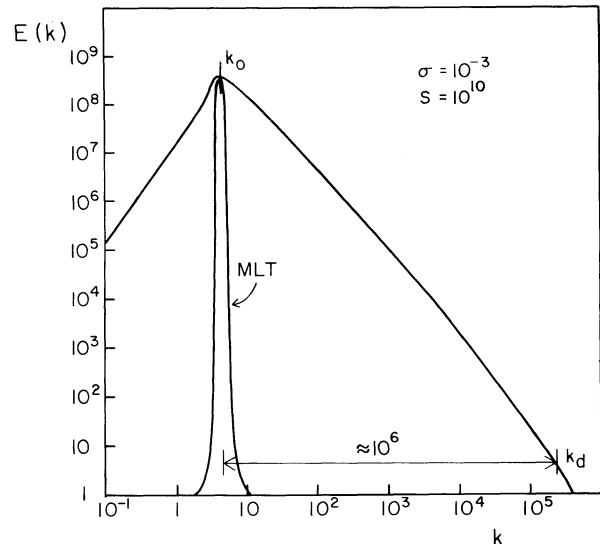

Fig. 1.—Turbulence energy spectrum $E(k)$ vs. k, for the case of convection. $E(k)$ and k are in units of χ^2/Λ and Λ^{-1}, respectively. The strength of convection is represented by $S = 10^{10}$. The Prandtl number is $\sigma = v/\chi$. (We recall that for water $\sigma = 6.6$, while for air $\sigma = 0.7$.) The figure corresponds to a rather inviscid fluid with $\sigma = 10^{-3}$. As expected, the Kolmogorov region is very extended, and the ratio between the largest and smallest eddies is about 10^6, as predicted by equation (28). As one can observe, the MLT curve is a poor approximation to the actual spectrum.
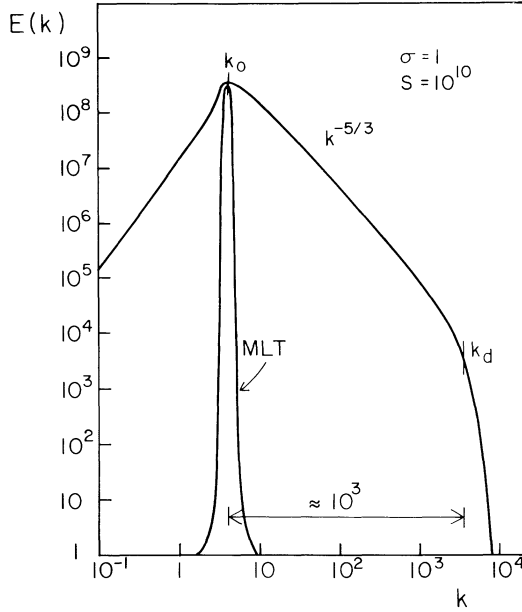
FIG. 2.—Same as Fig. 1, but for a viscosity 10^3 larger, $\sigma = 1$, e.g., air. The spectrum is narrower than in Fig. 1, but the MLT is still a poor approximation.

efficiencies, as

$$\frac{\ell_0}{\ell_d} \sim \sigma^{-3/4} S^{3/8} \sim \sigma^{-3/4}[A^2(\nabla - \nabla_{ad})]^{3/8} , \qquad (28)$$

where σ is the viscosity v in units of χ (for air $\sigma = 0.7$, for water $\sigma = 6.6$, while for stellar interiors σ is about 10^{-9}; Massaguer 1990). In Figures 1–3 we exhibit the dependence of the spectrum $E(k, v)$ on viscosity by keeping the convective strength S constant ($S = 10^{10}$) while increasing the viscosity. As one can see, as v increases, the range of the spectrum of eddies is
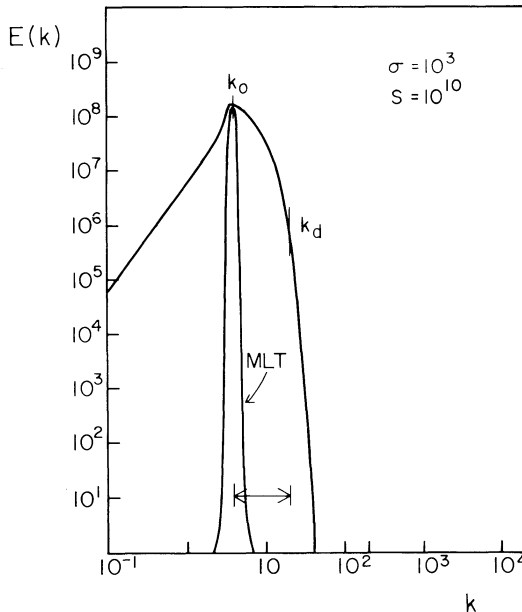

FIG. 3.—Same as Fig. 1, but for a viscosity 10^6 times larger, $\sigma = 10^3$. This value of the Prandtl number σ would correspond to a substance like oil. As one can see, the spectrum of eddies is extremely reduced with respect to that of Fig. 1. The MLT has become a more realistic approximation.

reduced according to the dependence on σ of equation (28), and $E(k)$ approaches a delta function as in equation (23). Thus, the MLT expression (23) pertains to the first of equations (27), i.e., it describes a system with a large viscosity. We have therefore seen that in the MLT the two basic ingredients of equation (12),

$$n_s(k, v) \quad \text{and} \quad E(k, v) , \qquad (29)$$

are assumed to be

$$n_s(k, v \to 0) \quad \text{and} \quad E(k, v \to \infty) , \qquad (30)$$

i.e., the MLT contains mathematical and physical inconsistencies. Mathematically, the two basic functions n_s and E are taken with opposite values of the parameter v. Physically, as stellar interiors have very small rather than very large v, the second of expressions (30) is singularly inadequate. The reduced spectrum of eddies represented by equation (23) misses the contribution of a large group of eddies to the transport of heat, thus leading to an underestimate of the convective flux. On this basis alone, it may be concluded that the true value of the convective flux F_c is

$$F_c > F_c^{MLT} . \qquad (31)$$

Equation (31) is borne out by stellar structure calculations, and by the direct numerical simulation of turbulent convection (Chan & Sofia 1989; Cabot et al. 1990).
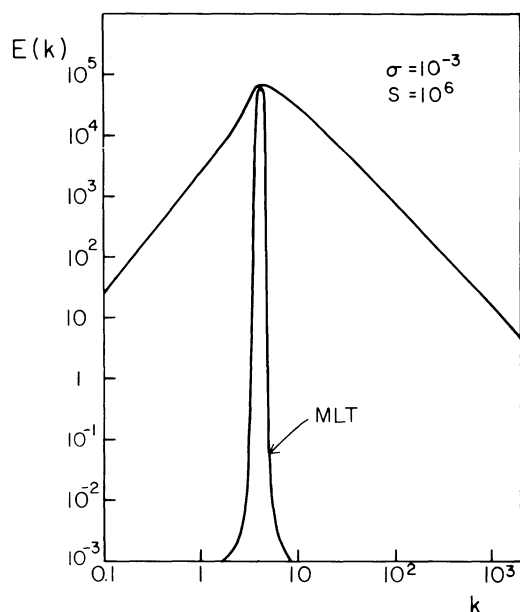
2.5. The New Convective Flux

Using equation (18) [with a model for the anisotropy x so that, in contrast to the MLT, the final result no longer contains x, since $x = (k\Lambda/\pi)^2 - 1$; see Canuto & Goldman 1985], we have solved equations (20)–(22) for $E(k, t)$ and then used the result to compute the convective flux given by equation (12). Because of the highly nonlinear nature of equations (20)–(22), the numerical solution of the problem is rather time-consuming. One begins with an initial trial function of the form $E(k, 0) \propto k^2 \exp(-ak^2)$ and time-evolves it using equation (20) until one reaches a stationary state, $E(k, \infty)$, which is the desired spectrum $E(k)$ to be used in equation (12). The most time-consuming part of the problem is the evaluation of the double integrals in the nonlinear transfer function (21).

As we have already discussed, highly viscous systems have a narrow spectrum of eddies and are easy to treat. On the contrary, the lower the viscosity (or σ), the wider the spectrum of eddies and the more time-consuming the solution of equations (20)–(22). Although the σ appropriate for stellar interiors may be as low as 10^{-9} (Massaguer 1990), we have chosen $\sigma = 10^{-3}$ as a reasonable representative value, since we found that when σ decreased further, $E(k)$ no longer changed significantly. Representative energy spectra $E(k)$ versus k for different values of S, or equivalently the convective efficiency, are shown in Figures 1–4.

With the new $E(k)$, we have computed the turbulent quantities of interest. In Table 1 we exhibit some representative values of the kinetic energy (eq. [11]), the turbulent viscosity, $v_t \equiv v_t(k_0, \infty)$ (eq. [22]), the new convective flux Φ (eq. [13]), and Φ^{MLT} (eq. [4]), as functions of $S \equiv 81\Sigma/2$, which in turn is simply related to the convective efficiency Γ (eq. [8]). Numbers in parentheses indicate powers of 10.

We have found that the values of the new convective flux Φ given in Table 1 can be fitted quite closely by the following

FIG. 4.—Same as Fig. 1, but for $S = 10^6$

FIG. 5.—Fitted function Φ (eq. [32]) compared with the numerical values (*open circles*).

expression

$$\Phi = a_1 \Sigma^m [(1 + a_2 \Sigma)^n - 1]^p , \qquad (32)$$

where Σ is defined by equations (5) and (6). The other coefficients are given by

$$a_1 = 24.868 , \quad a_2 = 9.7666 \times 10^{-2} , \qquad (33)$$
$$m = 0.14972 , \quad n = 0.18931 , \quad p = 1.8503 .$$

To highlight the difference with the MLT, in Figure 5 we plot $\Omega(\Sigma)$ versus Σ, where

$$\Omega(\Sigma) = \frac{\Phi}{\Phi^{MLT}} . \qquad (34)$$

As one can see, for large convective efficiencies, $\Omega(\Sigma)$ becomes a constant, Ω_∞, with the value

$$\Omega_\infty = 9.786 . \qquad (35)$$

See also Cabot et al. (1990, especially Fig. 17*a*).
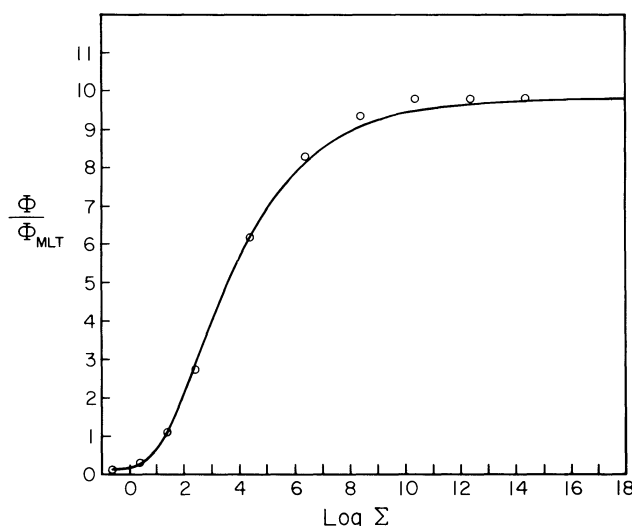
TABLE 1
RESULTS OF THE NEW MODEL[a]

log S	KE	v_t	Φ	Φ^{MLT}	C
4	5.26(3)	4.97	39.9	14.6	0.2241
6	8.78(5)	59.0	1.07(3)	1.73(2)	0.2145
8	9.83(7)	6.07(2)	1.46(4)	1.76(3)	0.2096
10	1.01(10)	6.15(3)	1.65(5)	1.77(4)	0.2083
12	1.01(12)	6.15(4)	1.73(6)	1.77(5)	0.2076
14	1.01(14)	6.15(5)	1.73(7)	1.77(6)	0.2143
16	1.01(16)	6.15(6)	1.73(8)	1.77(7)	0.2308

NOTE.—We note that the viscous dissipation rate,

$$\epsilon = 2v \int_0^\infty k^2 E(k) dk \quad (\text{ergs g}^{-1} \text{ s}^{-1}),$$

can easily be evaluated from Table 1, since $\epsilon/\epsilon_0 = S\Phi$, where $\epsilon_0 = \chi^3 \Lambda^{-4}$.

[a] Here $S \equiv 81\Sigma/2$, with Σ given by equation (5). The turbulent kinetic energy $\frac{1}{2}v_t^2 = $ KE, is in units of $(\chi/\Lambda)^2$; the turbulent viscosity, v_t, is in units of χ; and the parameter C is defined in equation (40). The ratio Φ/Φ^{MLT} is represented in Fig. 5.

2.6. *Solution of the Equations when the Total Flux Is Given*

Using the new expression for F_c, the relation that replaces equation (9) is

$$a_0 \Omega(\Gamma)\Gamma^3 + \Gamma^2 + \Gamma - \delta = 0 . \qquad (36)$$

The MLT result corresponds to $\Omega(\Gamma) = 1$. Equation (36) is therefore the new equation to be solved: for a given value of the thermodynamic quantity δ, it yields the value of Γ or, alternatively, the value of $\nabla - \nabla_{ad}$, as a function of $\nabla_r - \nabla_{ad}$ which is considered known.

2.7. *The Turbulent Pressure*

In the presence of strong turbulence, the pressure derived from the hydrostatic equilibrium equation p_{hydr} is related to the thermodynamic pressure $p_{th} = p_{gas} + p_{rad}$ by

$$p_{hydr} = p_{th} + p_{turb} , \qquad (37)$$

where p_{turb} is the contribution due to the turbulent motion. Due to the lack of a turbulence model to calculate the turbulence spectrum, it has been customary to parameterize p_{turb} as

$$p_{turb} = A_* \rho c_s^2 , \qquad (38)$$

where c_s is the speed of sound and A_* is an empirical constant assumed to be of order unity. Needless to say, this is not a completely satisfactory approach.

From the theory of turbulence it is known that (Batchelor 1953)

$$p_{turb}^2 = \rho^2 (8\pi^2)^{-1}$$
$$\times \iint E(k')E(k'') |k' - k''|^{-4} \sin^4 \theta \, d^3k' \, d^3k'' , \qquad (39)$$

where θ is the angle between k' and k''. For a justification of equation (39) see equation (58). Using the $E(k)$ derived from the solution of equations (20)–(22), we have computed expression (39). To make the results manageable, we write them in terms of the turbulent kinetic energy $\frac{1}{2}v_t^2$ given in Table 1, i.e.,

$$p_{turb} = 2C(\tfrac{1}{2}\rho v_t^2) \qquad (40)$$

The dimensionless parameter C is given in Table 1.

For large values of S, one can derive a simple formula relating the thermodynamic pressure to the total hydrostatic pressure. As one observes from Table 1, we have in good approximation

$$\tfrac{1}{2}v_t^2 = (\chi/\Lambda)^2 S . \tag{41}$$

Since from equations (7) and (5), $S = 162A^2(\nabla - \nabla_{ad})$, using the second part of equation (6), one obtains

$$p_{turb} = 2C\rho(g\Lambda^2/H_p)(\nabla - \nabla_{ad}) , \tag{42}$$

where the pressure used to define H_p is the total hydrostatic pressure. Dividing equation (42) by p_{hydr}, we further derive

$$p_{th} = p_{hydr}[1 - 2C(A/H_p)^2(\nabla - \nabla_{ad})] . \tag{43}$$

This is, however, not the final expression, since in the presence of turbulent pressure ∇_{ad} is given by (CG68, p. 295).

$$\nabla_{ad} = \nabla_{ad}^*(d \ln p_{th}/d \ln p_{hydr}) , \tag{44}$$

$$\nabla_{ad}^* = (\Gamma_2 - 1)/\Gamma_2 , \tag{45}$$

which, if substituted in equation (43), transforms it into a differential equation in the variable

$$u \equiv p_{hydr}/p_{th} , \tag{46}$$

namely (with $dp_{hydr}/dz = g\rho$),

$$f(z)\frac{du}{dz} + g(z)u - 1 = 0 , \tag{47}$$

where

$$f(z) = 2C\nabla_{ad}^* H_p(\Lambda/H_p)^2 , \tag{48}$$

$$g(z) = 1 - 2C(\nabla - \nabla_{ad}^*)(\Lambda/H_p)^2 . \tag{49}$$

The solution of equation (47) yields the desired function

$$p_{th} = p_{th}(p_{hydr}) . \tag{50}$$

2.8. *The Mixing Length Λ and Compressibility Effects*

In this section we shall present a set of arguments that lead us to propose that the phenomenon of "vertical stacking" of the turbulent eddies may be represented by the expression (z is the distance from the top of the convective zone)

$$\Lambda = z \tag{51}$$

as an alternative to the traditional

$$\Lambda = \alpha H_p . \tag{52}$$

We begin by asking which physical phenomenon has motivated the introduction of equation (52). Since H_p is smallest at the top of the convective zone and becomes larger with increasing depth, equation (52) represents the phenomenon of "vertical stacking" of the eddies in the CZ: convective eddies are assumed to be smallest near the top and larger deep in the interior. Is this effect real, and what is it due to? First, we discuss the fact that this is a phenomenon peculiar to convective turbulence and not, for example, to mechanically driven turbulence; then we discuss the fact that vertical stacking is caused by nonlinear compressibility effects (and not by the nonlinear interactions among eddies). This leads us to conclude that equation (52) tries to account for what the original formulation did not contain, i.e., compressibility effects, and is therefore a sensible thing to do. However, we shall also argue

that equation (51) may achieve the same goal with the considerable advantage that it contains no adjustable parameters.

First argument.—In an incompressible treatment of convective turbulence, the dimensionful physical variables are

$$g, \alpha, \beta, \nu, \chi . \tag{53}$$

With them, one can construct a unit of length, e.g.,

$$\ell \sim (\nu^2/g)^{1/3} \quad \text{or} \quad (\chi^2/g)^{1/3} . \tag{54}$$

However, in a nearly inviscid interior of a star, the large eddies (the dimensions of which are of the order of the size of the system) are so widely separated (in k-space) from the smaller eddies, or, alternatively, the range of eddies sizes is so large (Fig. 1), that viscosity does not really enter the problem, and so there is no length scale provided by the system. Furthermore, in the limit of high convective efficiency, χ does not enter the problem; see equations (3) and (4) and equation (32).

Monin & Obukhov (1954, cited in Priestley 1959, p. 40) were the first to point this out by stating that purely thermal turbulence is "self-patterning": there being no natural scale provided by the independent parameters of the problem, the length Λ cannot be written as a multiple of an intrinsic length that does not exist. This argument by itself would seem to suggest that under the conditions of "self-patterning," the only length is indeed the distance z, and so equation (51) follows.

To make the point even clearer, let us consider a physical situation in which turbulence is generated not by convection but by a wind, i.e., a mechanically rather than thermally driven turbulence (for example, the atmosphere of the Earth at night when there is a temperature inversion and thus no convection). Under these circumstances, observations (Kaimal et al. 1972) indicate that the largest scales of mechanical turbulence are considerably smaller than in the corresponding convective case: large-scale mechanical turbulence is inhibited because fluctuations would spend too much energy in working against gravity. Stated differently, large-scale fluctuations are stable. Therefore, mechanical turbulence consists mostly of small-scale eddies, and it has a local character, so that Λ *cannot depend explicitly on the distance from the surface* (Monin & Yaglom 1975) and it cannot be written as in equation (51).

On the other hand, the opposite is true in the presence of thermal stratification (i.e., convection), where observational data indicate that large fluctuations become unstable, the spectrum of eddies is wide (Fig. 1), the phenomenon is no longer local in character, and Λ must now depend on z.

Second argument.—Here we shall show that the equations we have used (and by extension the MLT equations) are based on the assumption that the fluid is incompressible.

Consider the basic equations (16), and note that the absence of the pressure term is due to the fact that under the condition of incompressibility the pressure is no longer an independent variable. Using the continuity equation,

$$\frac{\partial \rho}{\partial t} + \nabla \cdot (\rho v) = 0 , \tag{55}$$

the incompressibility condition, $\rho = $ constant, is equivalent to

$$\nabla \cdot v = 0 , \tag{56}$$

or

$$k \cdot v(k) = 0 , \tag{57}$$

i.e., only transverse waves are allowed. No longitudinal or

sound waves can enter the problem, or, stated differently, $c_s \to \infty$. Taking now the curl of equation (15a) and using equation (56), the pressure can be expressed in terms of the velocity field via the Poisson equation

$$\nabla^2 p(x) = -\rho \frac{\partial^2}{\partial x_i \partial x_j} v_i v_j \qquad (58)$$

(since $p \propto v^2$, we have $p^2 \propto v^4 \propto E^2$, i.e., eq. [39]). Substituting equation (58) into the Navier-Stokes equations, the pressure term becomes part of the nonlinear terms represented by the second term in equation (16a), which means that in *incompressible convection, pressure is not an independent variable that can be used to construct a unit of length.* One is therefore faced with a dichotomy: mathematically, the adoption of equation (56) leads to considerable simplifications of an extremely complicated nonlinear problem; physically, however, stellar interiors are compressible, and thus equation (56) cannot be true. The solution would be to tackle the fully compressible problem: although the formalism has recently become available (Hartke, Canuto, & Alonso 1988a), detailed results have yet to be obtained, partly because of the intimidating nature of the equations that replace equation (21). (Results of numerical simulations are available, but they cannot yet be linked to complex stellar structure codes; see Cloutman 1979; Massaguer & Zahn 1980; Gilman & Glatzmeier 1981; Hurlburt, Toomre, & Massaguer 1984; Gilman & Miller 1986; Chan & Sofia 1989; Stein & Nordlund 1989; Hossain & Mullan 1990). The pragmatic alternative has been the adoption of an incompressible formalism (like the MLT or the present model) with compressibility effects introduced via the mixing length Λ (and of course the adiabatic gradient), a procedure that, while not entirely satisfactory, has the merit of simplicity provided that it does not create more problems than it tries to solve.

The next relevant question is: can one prove that equation (52) does indeed incorporate compressibility effects? Since we believe that this point is important, we shall discuss it here. Consider the growth rate (18) in the limit when v and χ do not enter the problem. We have

$$n_s = [g\alpha\beta x/(1 + x)]^{1/2} , \qquad (59)$$

i.e., the stability analysis under the condition of incompressibility provides a natural unit of time, *but not of length.* Consider now the case of a compressible fluid, and let ω be the frequency ($-\text{Im } \omega$ is the growth rate). The equation to be solved is a second-order differential equation (Chimonas 1970) which requires the specification of the velocity of sound c_s and density ρ as functions of z. In the case of an isothermal profile, with constant c_s, such an equation simplifies considerably (Spiegel & Moore 1964; Einaudi 1980). In terms of $\Omega \equiv \omega^2$,

$$\Omega^2 - \Omega c_s^2 k^2 (1 + \gamma^2 g^2/4k^2 c_s^4) + k_\perp^2 f^2 c_s^2 = 0 , \qquad (60)$$

where f is the Brunt-Väisälä frequency ($f^2 = -g\alpha\beta$). For an incompressible fluid, $c_s^2 \to \infty$, equation (60) reduces to equation (59). From equation (60) it is seen that a unit of length is naturally provided by the second term in the parentheses,

$$\ell = c_s^2/\gamma g = p/g\rho = H_p , \qquad (61)$$

which is precisely the pressure scale height.

In conclusion, we can summarize the problem in the following manner:

1. Incompressibility is assumed because it entails a considerable mathematical simplification in the treatment of turbulence.

2. Stellar interiors are, however, compressible (finite sound speed), and efforts must therefore be made to incorporate this feature into the problem.

3. Early work by Chan, Sofia, & Wolff (1982) and recent work by Hossain & Mullan (1990) has shown that nonlinear compressibility effects act quite separately from the nonlinear interactions among eddies: the former are responsible for the "vertical stacking" of the eddies whereby convective eddies are on average smaller at the top of the CZ and grow increasingly larger with depth; the nonlinear interactions among eddies are in turn responsible for the convective transport of heat.

4. The MLT treats the nonlinear interactions among eddies with a one-eddy, incompressible model with compressibility partially accounted for through equation (52). The procedure is incomplete at best, since the presence of the free parameter α considerably weakens the predictive power of the model.

5. The present model improves over the MLT in the treatment of the nonlinear interactions and of the compressibility effects because equation (51) accounts for the "vertical stacking" without introducing the parameter α.

6. When the growth rate and the energy spectrum $E(k)$ needed to compute F_c (eq. [12]) will be derived from a fully compressible turbulence model, H_p will emerge as the natural unit of length: in that case, there will be no need for an α, since all lengths will be measured in units of H_p. (See § 3.8.)

3. APPLICATION OF THE NEW MODEL TO STELLAR STRUCTURES

3.1. *The Numerical Scheme*

Since in the new model equation (36) is no longer a cubic relation as in the MLT case, it is convenient, using equation (3) and the equation for the radiative transfer $F_{rad} = KTH_p^{-1}\nabla$, to write the total flux,

$$F_{total} = F_c + F_{rad} , \qquad (62)$$

as

$$\nabla = (\nabla_r + \Phi\nabla_{ad})(1 + \Phi)^{-1} , \qquad (63)$$

where Φ is given by equations (32) and (33). Since Φ depends on S, i.e., on ∇ itself, a simple iterative procedure (using log variables) from a trial value of $\nabla - \nabla_{ad}$ will converge rapidly, primarily because of the monotonic behavior of the Φ versus S function. From the point of view of an evolutionary code, we found it even more expedient to compute a matrix of values of $\log(\nabla - \nabla_{ad})$ as a function of $\log A$ and of $\log(\nabla_r - \nabla_{ad})$, where A is given by equation (6), and then bilinearly interpolate on the matrix given in Table 2.

Next, at each point of the structure, the nonlocal nature of the relation $\Lambda = z$ requires the knowledge of the thickness of the convective region from that point to the surface. Depending on the structure of the evolutionary code, we suggest two feasible solutions. The most obvious one is to perform a Newton-Raphson integration for the whole stellar structure, up to the base of the optical atmosphere, since in this way a trial determination of the upper boundary of the convective region is always available. The results presented in this paper have been obtained using such a scheme (Mazzitelli 1989a and references therein).

The new formalism can also be easily implemented in evolutionary codes in which grids of atmospheres and sub-atmospheres (where overadiabatic convection is usually restricted) are integrated via a Runge-Kutta scheme starting from the surface. In fact, in the downward integration, as soon

TABLE 2
Overadiabatic Excesses[a]

-4.000 -5.0000 -4.0000 -3.0000 -2.0000 -1.0000 0.0000
1.000 2.0000 3.0000 4.0000 5.0000 6.0000 6.9990

-3.5000 -5.0000 -4.0000 -3.0000 -2.0000 -1.0000 0.0000
1.0000 2.0000 3.0000 4.0000 5.0000 5.9990 6.9396

-3.0000 -5.0000 -4.0000 -3.0000 -2.0000 1.0000 0.0000
1.0000 2.0000 3.0000 4.0000 4.9990 5.9396 6.5743

-2.5000 -5.0000 -4.0000 -3.0000 -2.0000 -1.0000 0.0000
1.0000 2.0000 3.0000 3.9990 4.9396 5.5743 6.0685

-2.0000 -5.0000 -4.0000 -3.0000 -2.0000 -1.0000 0.0000
1.0000 2.0000 2.9990 3.9396 4.5743 5.0685 5.5711

-1.5000 -5.0000 -4.0000 -3.0000 -2.0000 -1.0000 0.0000
1.0000 1.9990 2.9396 3.5743 4.0685 4.5711 5.1103

-1.0000 -5.0000 -4.0000 -3.0000 -2.0000 -1.0000 0.0000
0.9990 1.9396 2.5743 3.0685 3.5711 4.1103 4.6841

-0.5000 -5.0000 -4.0000 -3.0000 -2.0000 -1.0000 -0.0010
0.9396 1.5743 2.0685 2.5711 3.1103 3.6841 4.2842

0.0000 -5.0000 -4.0000 -3.0000 -2.0000 -1.0010 -0.0604
0.5743 1.0685 1.5711 2.1103 2.6841 3.2842 3.9030

0.5000 -5.0000 -4.0000 -3.0000 -2.0010 -1.0604 -0.4257
0.0685 0.5711 1.1103 1.6841 2.2842 2.9030 3.5350

1.0000 -5.0000 -4.0000 -3.0010 -2.0604 -1.4257 -0.9315
-0.4289 0.1103 0.6841 1.2842 1.9030 2.5350 3.1764

1.5000 -5.0000 -4.0010 -3.0604 -2.4257 -1.9315 -1.4289
-0.8897 -0.3159 0.2842 0.9030 1.5350 2.1764 2.8246

2.0000 -5.0010 -4.0604 -3.4257 -2.9315 -2.4289 -1.8897
-1.3159 -0.7158 -0.0970 0.5350 1.1764 1.8246 2.4776

2.5000 -5.0604 -4.4257 -3.9315 -3.4289 -2.8897 -2.3159
-1.7158 -1.0970 -0.4650 0.1764 0.8246 1.4776 2.1342

3.0000 -5.4257 4.9315 -4.4289 -3.8897 -3.3159 -2.7158
-2.0970 -1.4650 -0.8236 -0.1754 0.4776 1.1342 1.7934

3.5000 -5.9315 -5.4289 -4.8897 -4.3159 -3.7158 -3.0970
-2.4650 -1.8236 -1.1754 -0.5224 0.1342 0.7934 1.4545

4.0000 -6.4289 -5.8897 -5.3159 -4.7158 -4.0970 -3.4650
-2.8236 -2.1754 -1.5224 -0.8658 -0.2066 0.4545 1.1171

4.5000 -6.8897 -6.3159 -5.7158 -5.0970 -4.4650 -3.8236
-3.1754 -2.5224 -1.8658 -1.2066 -0.5455 0.1171 0.7807

5.0000 -7.3159 -6.7158 -6.0970 -5.4650 -4.8236 -4.1754
-3.5224 -2.8658 -2.2066 -1.5455 -0.8829 -0.2193 0.4451

5.5000 -7.7158 -7.0970 -6.4650 -5.8236 -5.1754 -4.5224
-3.8658 -3.2066 -2.5455 -1.8829 -1.2193 -0.5549 0.1100

6.0000 -8.0970 -7.4650 -6.8236 -6.1754 -5.5224 -4.8658
-4.2066 -3.5455 -2.8829 -2.2193 -1.5549 -0.8900 -0.2246

6.5000 -8.4650 -7.8236 -7.1754 -6.5224 -5.8658 -5.2066
-4.5455 -3.8829 -3.2193 -2.5549 -1.8900 -1.2246 0.5589

7.0000 -8.8236 -8.1754 -7.5224 -6.8658 -6.2066 -5.5455
-4.8829 -4.2193 -3.5549 -2.8900 -2.2246 -1.5589 -0.8929

7.5000 -9.1754 -8.5224 -7.8658 -7.2066 -6.5455 -5.8829
-5.2193 -4.5549 -3.8900 -3.2246 -2.5589 -1.8929 -1.2268

8.0000 -9.5224 -8.8658 -8.2066 -7.5455 -6.8829 -6.2193
-5.5549 -4.8900 -4.2246 -3.5589 -2.8929 -2.2268 -1.5605

8.5000 -9.8658 -9.2066 -8.5455 -7.8829 -7.2193 -6.5549
-5.8900 -5.2246 -4.5589 -3.8929 -3.2268 -2.5605 -1.8941

9.0000 -10.2066 -9.5455 -8.8829 -8.2193 -7.5549 -6.8900
-6.2246 -5.5589 -4.8929 -4.2268 -3.5605 -2.8941 -2.2277

9.5000 -10.5455 -9.8829 -9.2193 -8.5549 -7.8900 -7.2246
-6.5589 -5.8925 -5.2268 -4.5605 -3.8941 -3.2277 -2.5612

10.0000 -10.8829 -10.2193 -9.5549 -8.8900 -8.2246 -7.5589
-6.8929 -6.2268 -5.5605 -4.8941 -4.2277 -3.5612 -2.8946

[a] In each block of values the first entry is the value of $\log A$; the following 13 entries are the values of $\log (\nabla - \nabla_{ad})$ corresponding to values of $\log (\nabla_r - \nabla_{ad})$ ranging from -5.0 to $+7.0$. (A more complete table is available through Bitnet to: Italo at Irmias.)

as the upper boundary of the convective region is reached, one can begin evaluating z. The only caution is that, since the subatmospheric temperature gradient is steeper than in the MLT case (see later), the grids of envelopes in the H-R diagram must be kept relatively narrow, and the mesh zoning in the overadiabatic region thinner.

Finally, to achieve completeness in the treatment of overadiabatic convection, one must include turbulence pressure. In principle, p_{turb} can be evaluated according to equation (42). However, for the purpose of numerical stability in the evaluation of ∇_{ad} (eq. [44]), we suggest using equations (46)–(49). A problem may arise, since pressure is a primary structural variable, from which the density is evaluated through an equation of state, so that a preliminary knowledge of p_{turb} is required, from which p_{gas}, ρ, ∇, and finally p_{turb} itself are computed. In the evolutionary code adopted in this paper, the problem is avoided, since the overadiabatic zone is included in the Newton-Raphson integrated region, the trial values of p_{turb} are stored at each mesh point, and the numerical iterations automatically lead to self-consistent convergence.

On the other hand, if one adopts an evolutionary code in which overadiabaticity is restricted to the Runge-Kutta integrated grids of envelopes, one will have to devise a workable scheme to deal with p_{turb}. A numerical iteration scheme can in principle be adopted (e.g., density is evaluated without accounting for p_{turb}, from which a trial value of p_{turb} is obtained, to be used to recompute the density, and so on until convergence is reached), but experience shows that the nonlinearity of overadiabatic convection is such that, at least in unsophisticated iterative schemes, convergence is rather slow. A first attempt at implementing this scheme did work but proved to be extremely time-consuming. In our opinion, only two solutions exist for the treatment of p_{turb}: either one switches to a full Newton-Raphson code up to the surface of the star (which is not a mammoth task, as experience shows), or one simply ignores p_{turb}, since, as will be shown later, there may be evolutionary phases in which the influence of p_{turb} is moderate.

3.2. The $\Lambda = \alpha H_p$ Case

Although we have given reasons to prefer equation (51) over (52), in a first attempt we adopt the relation $\Lambda = \alpha H_p$ with the new model for the convective flux (eq. [32]). This procedure allows us to isolate and quantify the effect of having taken into account all the eddies rather than just the largest ones, as in the MLT. For consistency reasons, we also neglect p_{turb}.

To fit the Sun, the new model requires $\alpha = 0.7$, with $Y = 0.27$ (Figs. 6 and 7, curve 2), while the standard MLT model requires $\alpha = 1.4$ (Figs. 6 and 7, curve 1). The depth of the convective region turns out to be almost identical in the two cases; this is no longer true, however, of the internal behavior of the gradients as well as of the temperature profiles (Figs. 8 and 9). The fact that the new model requires a smaller value of α is a direct consequence of the fact that the new convective flux is much larger than the MLT values. The new value of $\alpha < 1$ is a welcome feature, since it implies that, along a convective "bubble," the pressure changes by a factor of 2 only, whereas the MLT model requires a change by a factor of 4, far less consistent with the underlying assumption of incompressibility.

A further consequence of $\alpha < 1$ is that, in the upper convective layers, the value of A is smaller than in the MLT case. This leads to a larger degree of overadiabaticity (Fig. 8, curve 2). The internal profile of temperature is also clearly changed (Fig. 9), and this leads to differences in the behavior of the speed of
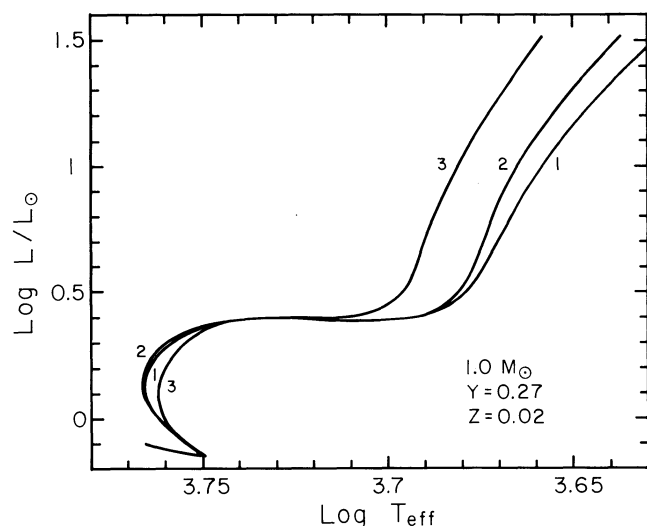
FIG. 6.—Evolutionary tracks in the H-R diagram for a 1 $M_\odot$ star, with $Y = 0.27$, $Z = 0.02$, for the three cases (1) MLT, $\Lambda = 1.4H_p$; (2) new theory, $\Lambda = 0.7H_p$, no turbulent pressure; (3) new theory, $\Lambda = z$, with turbulent pressure.

sound c_s close to the surface; the possible influence of these differences in the computation of solar pulsational modes remains to be investigated.

As can be seen from Figure 6, the evolutionary phases of the Sun up to midway along the red giant branch are not significantly different in cases 1 and 2. Almost the same is true for the evolution of a globular cluster star of 0.8 $M_\odot$, $Y = 0.23$, and $Z = 0.001$ (Fig. 12). From these two evolutionary tracks, a common feature emerges: the slope of the red giant branch is somewhat steeper with the new theory, and the red giants slightly hotter. A more detailed analysis of the temperature and density profiles will be presented after discussing the results arising from the full theory (see § 3.3).
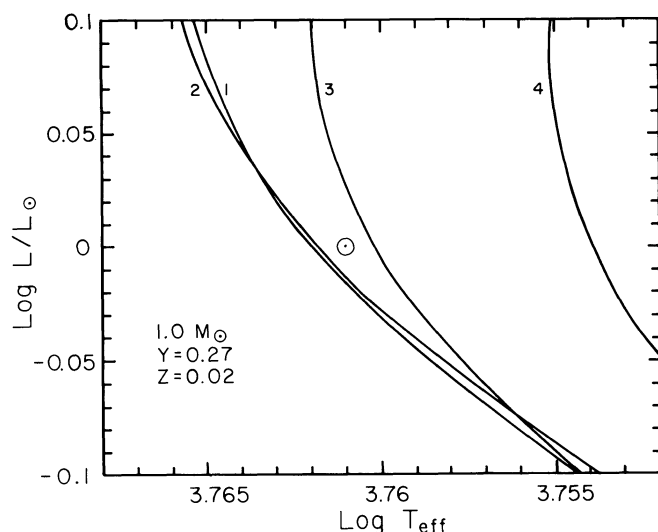

FIG. 7.—Curves 1, 2, and 3; same as Fig. 6, but for the immediate neighborhood of the present position of the Sun, marked by the solar symbol. Curve 3, corresponding to the model without free parameters, fits the observed T_{eff} within 0.2%. Curve 4 corresponds to the standard MLT with $\Lambda = z$: it fails to fit T_{eff} of the Sun by $\sim 2\%$.

In conclusion:

1. The new model describes turbulence in a more realistic way than the MLT, for it includes the large spectrum of eddies that characterize a nearly inviscid medium such as a stellar interiors.

2. The new model can easily be implemented in existing stellar codes.

3. The new model requires $\alpha < 1$, which is a welcome feature on its own right.

4. The new model gives rise to several differences with respect to the MLT; on the basis of items 1–3 above, they are expected to be in the right direction.

When all the above considerations are taken together, they suggest that the new expression for the convective flux, equation (32), even with the $\Lambda = \alpha H_p$ expression, is to be preferred to the standard MLT.

3.3 The $\Lambda = z$ Case

In this section we shall explore the new relation $\Lambda = z$, where z is the distance between the point at which the overadiabatic gradient is to be computed and the top of the convective zone.

In this framework it is clear that, at least for the more external convective layers, the values of z can be orders of magnitude smaller than H_p. The corresponding values of A are thus much smaller than in the previous cases (§ 3.2), with the consequence that overadiabaticity is more strongly peaked toward the surface of the convective zone. This result is indeed borne out by detailed numerical computations: as seen from Figure 8, for a 1 $M_\odot$ star, the peak value of $\nabla - \nabla_{ad}$ for case 3 can be twice as large as in cases 1 and 2.

A large value of $\nabla - \nabla_{ad}$ means that p_{turb} can no longer be ignored (see eq. [42]). Our numerical computations indicate that, in the case of the Sun, p_{turb} can easily reach 10% of the total pressure, while for red giants it can be as large as 40%–50%. As for the adiabatic gradient (eq. [44]), it can increase up to a maximum of 3%–5% for a 1 $M_\odot$, while for a red giant the maximum increase can be 15%–20%. On the basis of these estimates, we concluded that it was necessary to account for p_{turb} in the computations (see Figs. 6–9).

Turbulence pressure acts in several ways. First, since it contributes to the total pressure, the part due to the gas pressure is reduced, and this leads to a lower density in the overadiabatic regions. This in turn leads to a decrease in the value of A (eq. [6]), and thus an increase in the degree of overadiabaticity is to be expected. However, in almost all the cases investigated in the present work, there is a phenomenon which almost exactly counteracts the previous effect. In fact, very close to the top of the convective zone the opacity decreases significantly because of the sharp drop in density (when approaching the surface of the star). The further decrease in density due to p_{turb} leads to an even faster decrease of the opacity and radiative gradient, which, in turn, tends to *lower* the overadiabaticity. The last effect of p_{turb} is to change the adiabatic gradient according to equation (44). In the overadiabatic region, the increase in the values of ∇_{ad} leads to a corresponding increase in the values of the convective gradient, and the surface of the star becomes cooler.

In practice, while the effect of p_{turb} results in a slight modification in the internal behavior of the gradients, the location of the evolutionary tracks in the H-R diagram is not severely changed.

3.4. Results

A basic requirement of any physical theory is that it should be able to make predictions and thus be falsifiable, which is possible only if the theory contains no adjustable parameters. The MLT does not satisfy this requirement, nor does the present theory if Λ is taken to be αH_p. On the contrary, the $\Lambda = z$ model is falsifiable: if it does not fit the Sun, it ought to be discarded.

The above conclusion needs to be further quantified, since not all of the remaining physics is fully understood. Notwithstanding phenomena such as rotation, magnetic fields etc., which may have small but perhaps detectable influence on observed surface parameters, there are other physical quantities such as opacities, thermodynamics, and nuclear reactions which are known to a finite accuracy only. For example, switching from the Cox & Stewart (1970) to the Los Alamos (Huebner et al. 1977) opacities, adopted for the present computations, forces an increase in the helium abundance of 2%–3% to fit the Sun's luminosity. Furthermore, when the new low-temperature opacities of A. D. Alexander (1990, private communication) are adopted, as in the present case, the surface temperature of the Sun changes again by 2%–3%, requiring a further adjustment of the value of α.

These examples imply that further improvements in the input physics may be expected to lead to modifications of the theoretical predictions of the order of a few percent, so that even the most reliable turbulent convection theory might yield, together with other present input physics, a T_{eff} for the Sun slightly different from the observed value. For these reasons, we decided that in the case of the Sun, a fit of T_{eff} within 1% would have to be considered a successful prediction of the new model.

For 1 $M_\odot$ we computed one more evolutionary track from the homogeneous main sequence up to midway along the red giant branch. Figure 6 shows the theoretical H-R diagram for the following three cases: (1) MLT, $\Lambda = 1.4H_p$; (2) new theory, $\Lambda = 0.7H_p$, and $p_{\text{turb}} = 0$; and (3) new theory, $\Lambda = z$, and $p_{\text{turb}} \neq 0$.

As already noted, the first two cases give nearly the same results, but with the advantage in case 2 that $\alpha < 1$. In the third case the general topology seems to be somewhat different. The beginning of the main-sequence phase coincides with the previous cases, the value of T_{eff} at the turnoff is somewhat lower ($\sim 1\%$), while T_{eff} in the red giant phase is 4%–5% larger. More interesting perhaps is Figure 7, which shows an enlargement of Figure 6 in the neighborhood of the present position of the Sun (represented by the solar symbol). The new theory (curve 3) fits the present position of the Sun within -10 K, or -0.2%. The results of the $\Lambda = z$ case without the turbulent pressure are not reported in Figure 7; they would have fitted the Sun within a similar accuracy, but with opposite sign, $+0.2\%$. An attempt to make the MLT more self-consistent by assuming $\Lambda = z$ was not successful, since it failed to fit the present solar T_{eff} by $\sim 2\%$ (Fig. 7, curve 4; see also Fig. 10, curve 3).

Given the previous discussion about the possible uncertainties in the input physics, the fit provided by curve 3 of Figure 7 is surprisingly good.

While this fit may be considered a strong argument in favor of the overall correctness of the model suggested here, a much more extensive analysis aimed at comparing theoretical evolutionary tracks with observational data must still be carried out to put the model on a firmer basis. For example, one should undertake the evaluation of extensive grids of theoretical isochrones to try to match the observed H-R diagrams of gobular and open clusters. In doing so, it will be necessary, however, to keep in mind that the vast majority of existing correlations between theoretical quantities (e.g., bolometric luminosities and effective temperatures) and observational quantities (e.g., magnitudes and colors) already contain elements of a chosen theoretical model. This implies that great care must be exercised in ensuring full consistency in the comparison process. The same is true for the case of correlations obtained by means of model atmospheres. In fact, the theoretical evaluation of the spectral distribution of the luminous flux from the surface of a star of given total luminosity and surface gravity requires the knowledge of the physical stratifications well below the optical atmosphere itself, down to Rosseland optical depths of the order of 10 or more, where overadiabatic convection, and thus the need for a theoretical model, comes into play.

Another interesting possibility is to use helioseismological data, since, as already noted, the internal behavior of the convective gradients predicted by the new theory is quite different from those of the MLT (Fig. 8). In the following section we shall discuss this point in more detail.

3.5. Temperature and Density Stratifications

For the present Sun the profile of the convective gradient ∇ at the top of the overadiabatic region is shown in Figure 8 for the three cases (1) MLT, $\Lambda = 1.4H_p$; (2) new theory, $\Lambda = 0.7H_p$ and $p_{\text{turb}} = 0$; (3) new theory, $\Lambda = z$, and $p_{\text{turb}} \neq 0$. On the basis of the discussions in §§ 3.2 and 3.3, it is not surprising to see that, when moving from the surface inward, the convective gradient of the new model sticks to the (virtual) radiative one much longer than in the MLT and/or case 2. This is due to the fact already mentioned that, since z is much smaller than H_p in this region, the value of A is also smaller and convection is significantly more overadiabatic. As z increases, it eventually becomes larger than H_p, at which point convection becomes less overadiabatic than in the MLT and/or case 2, and the convective gradient begins to decrease faster.
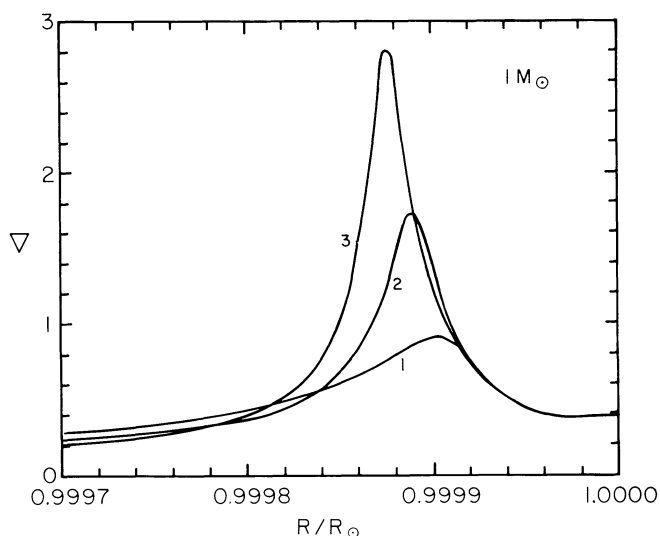

Fig. 8.—Behavior of the convective gradients close to the surface of the Sun. The three cases are the same as in Fig. 6. The case without free parameters, curve 3, shows a much larger degree of overadiabaticity than the other cases; note, however, that even curve 2 is more overadiabatic than the standard MLT.

The peaked behavior of the ∇ versus R function in a narrow subsurface deserves some comments. Since in these layers the values of z are rather small, any uncertainties in the determination of the exact point at which convection ceases, leads to similar uncertainties in the values of z in a critical region. In all the cases considered in this paper, this problem does not arise since the upper boundary of convection coincides almost identically with the bottom of the optical subatmosphere; however, situations may arise (e.g., very high luminosity red giants and supergiants), in which the radial distance between the top of the convective zone and the base of the photosphere is not negligible. Consistent with the boundary conditions underlying both the MLT, the present theory and practically all available models of turbulent convection, both velocity *and* acceleration (buoyancy) vanish when $\nabla - \nabla_{ad}$ vanishes (see CG68, eqs. [14.118–14.121]); this means that convective overshooting should, in principle, not be allowed; it is nevertheless worth noticing that, at least for the case of supergiants, the possible existence of even a small amount of convective overshooting (expected on physical grounds) would pose the question of where to start evaluating z, that is, from the top of the overshooting layers or from the layer where the Schwarzschild criterion $\nabla - \nabla_{ad} \to 0$ is satisfied?

From the point of view of internal temperature profiles (Fig. 9), the merging of the surface temperatures of the three models is the consequence of a spontaneous, although quite surprising, fine tuning. In Figure 9 the temperature profiles are shown for the same three cases as in Figure 8, but for a deeper region, down to the point where overadiabaticity has disappeared.

Starting from the left and moving outward, at first the temperatures coincide, since in the deep layers they are mainly determined by the overall stellar properties. As soon as a small degree of overadiabaticity develops, in the MLT case the overadiabatic gradient begins to grow slightly larger than in the new model and thus the temperature begins to decrease sharply. A maximum difference in temperature of $\Delta \log T \sim 0.1$ between the MLT and the new theory is attained in the region close to the surface; then the sharper increases of the overadiabatic gradient obtained with the new model give rise
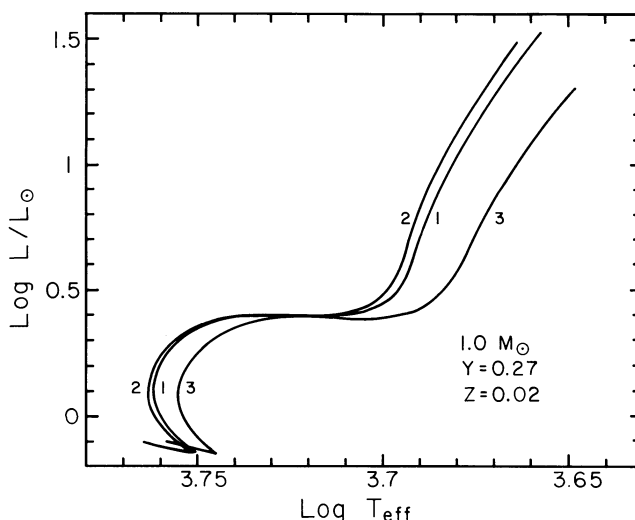
FIG. 10.—Evolutionary tracks in the H-R diagram for a 1 $M_\odot$ star, with $Y = 0.27$ and $Z = 0.02$, for (1) new theory, $\Lambda = z$, with turbulent pressure; (2) new theory, $\Lambda = z$, no turbulent pressure; and (3) MLT, $\Lambda = z$, no turbulent pressure.

to a sharper drop in temperature; eventually, the temperatures merge at the surface.

In practice, the interplay of the gradients is such that the final surface temperature difference between the two extreme cases is no more than 2% of the maximum internal temperature difference that is attained in the subsurface. This is not particularly relevant to the solar model, since a better choice of α in the MLT case would have fitted the same T_{eff} as in the $\Lambda = z$ case. It is, however, more relevant in the red giant case, where the surface temperature differences between the MLT and the new theory are not negligible. These differences correspond to less than 10% of the maximum temperature differences inside the corresponding structures, near the peak of the overadiabatic gradient.

As for the thickness of the whole convective region for the Sun, it is easy to understand that, since the differences among the three above treatments are limited to the thin subsurface layers, the conditions at the bottom of the convective envelope are not affected, and the total thickness is the same in all cases, consistent with the requirements from helioseismology.

3.6. *Other Results: Younger Globular Clusters?*

It may be of interest to compare tracks with and without turbulence pressure, to compute MLT tracks with $\Lambda = z$, as well as to apply the new model to a globular cluster star. The three tracks shown in Figure 10 correspond to the following: (1) new theory, $\Lambda = z$, $p_{turb} \neq 0$; (2) new theory, $\Lambda = z$, $p_{turb} = 0$; and (3) MLT, $\Lambda = z$, $p_{turb} = 0$. As can be seen, in the absence of turbulent pressure, the surface temperature is $\sim 1\%$ hotter in the red giant region, an effect whose neglect may not significantly affect the comparison with observational data. See also Figure 7.

Density profiles inside the overadiabatic region are different in the various cases, as shown in Figure 11, where we exhibit four different cases. The main conclusion is that the more complete the model, the more pronounced is the density inversion in the overadiabatic region.

The new model has also been applied to a globular cluster star, namely, a 0.8 $M_\odot$ star with $Y = 0.23$ and $Z = 10^{-3}$. The
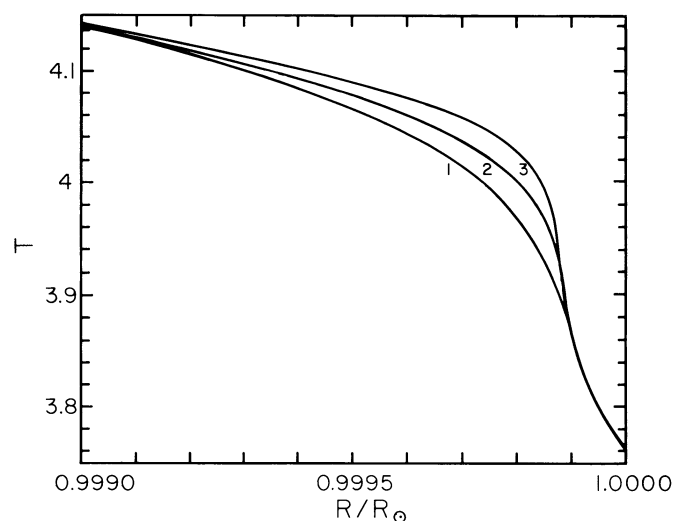

FIG. 9.—Behavior of the temperature for the same three cases described in Fig. 6. The relatively large differences in temperature in the immediate subsurface layers are reset both at the surface and toward the interior of the star.
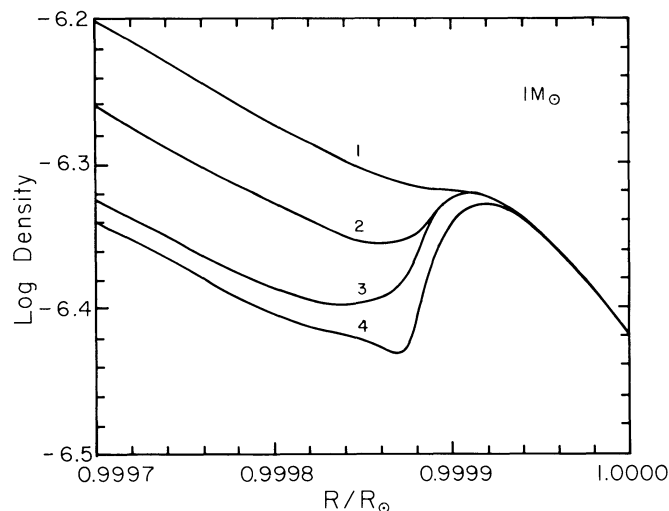
FIG. 11.—Behavior of density as a function of radius close to the surface of the Sun, for the four cases (1) MLT, $\Lambda = 1.4H_p$, no turbulent pressure; (2) new theory, $\Lambda = 0.7H_p$, no turbulent pressure; (3) new theory, $\Lambda = z$, no turbulent pressure; and (4) new theory, $\Lambda = z$, with turbulent pressure. As can be appreciated, the more complete version of the new model, curve 4, predicts a density inversion larger than any of the previous models.

results shown in Figure 12 correspond to three different cases. The MLT and case 2 are similar, as for the Sun, with case 2 giving a slightly hotter red giant. Surprisingly enough, however, the full case 3 gives rise not only to a cooler main-sequence star (up to 6%–7% in T_{eff} at the turnoff) but also to a cooler red giant, rather than to a hotter one as for the Sun (Fig. 6). Curve 3 implies that to fit the observed colors of the turnoff of globular clusters, a somewhat larger mass, and thus a younger age, would be required, a result that might have interesting cosmological consequences.

3.7. Future Work: Stellar Structure

Although the following list is not exhaustive, we cite some of the main lines of research that may be undertaken in the future.
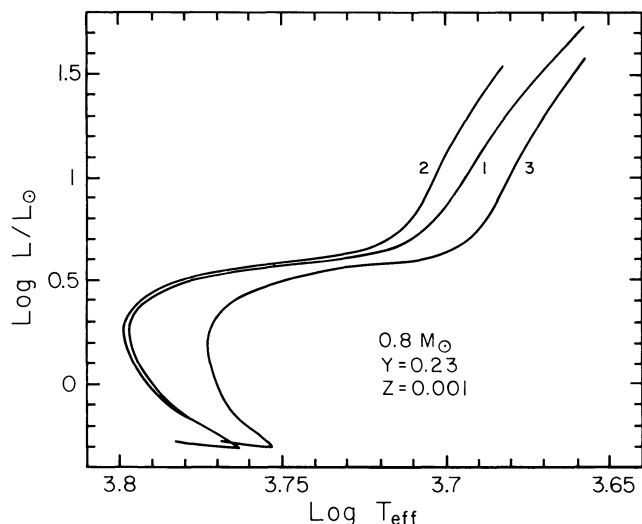

FIG. 12.—Evolutionary track in the H-R diagram for a typical globular cluster star of 0.8 $M_\odot$, with $Y = 0.23$ and $Z = 0.001$. The three cases are as in Fig. 6. The treatment without free parameters, curve 3, seems to give rise to at least "reasonable" evolutionary features also in this case.

1. The low-mass main-sequence stars are known to be cooler than theoretical models predict (Burrows, Hubbard, & Lunine 1989). At least in part, this is probably due to the fact that the relatively large density in the subatmospheres of these stars does not allow a sufficient degree of overadiabaticity to develop, at least within the MLT framework. Since in the present theory a peak of overadiabaticity is expected to develop also for these structures, it is quite likely that the new theory might yield lower surface temperatures and thus better agreement with the data.

2. A correct theoretical explanation of the blue edge of the instability strips for both helium-rich and hydrogen-rich white dwarfs requires a convective flux in excess of that provided by the standard MLT (Tassoul, Fontaine, & Winget 1990). While this is difficult to achieve within the MLT with the same value of α that fits the Sun, we have already seen that the new theory (Fig. 5) naturally yields convective fluxes up to 10 times larger than the MLT values. In general, all the cases in which surface convection is relevant in determining the pulsational behavior of stars (e.g., RR Lyrae stars, Mira variables, etc) can be affected by the new theory.

3. For horizontal-branch stars, theory predicts that at the end of the central helium-burning phase large-scale mixing episodes, usually called "breathing pulses," should occur. Since the observational luminosity functions do not agree with the evolutionary times computed when the breathing pulses occur, it has been suggested that the mixing time scale of semiconvection may be so long as to inhibit these final pulses (Caputo et al. 1989). Within the MLT framework, however, the convective velocities are so large that inhibition of the breathing pulses seems impossible. On the other hand, the new theory prediction of much lower convective velocities may naturally resolve the breathing pulse problem.

4. The lower values of the convective velocities also imply that convective overshooting (if any) should be definitely smaller than that predicted by the MLT (Bressan, Bertelli, & Chiosi 1986).

5. It has been known for quite some time that the so-called third dredge-up can give rise to carbon stars only if the surface convection is very efficient. Actually, in the standard MLT, a value of at least $\alpha = 1.5$ is required (Lattanzio 1989) to produce the desired effect. The new theory predicts larger convective fluxes which, from this point of view, correspond to MLT values of α even larger than 1.5, so that it can probably help in naturally explaining the carbon star phenomenon.

6. During the "second dredge-up," intermediate-mass stars ($\leq 8–9 M_\odot$) show a large degree of overadiabaticity for most of their structure, all the way down to the base of the convective envelope (Mazzitelli 1989b). Within the new theory, the structure of these stars is likely to be substantially different from that in the MLT, although in the absence of detailed calculations it is difficult to anticipate in which direction.

7. The onset of mass exchange in binary stars is largely dependent on the gravothermal reaction of the subsurface overadiabatic layers to mass loss (D'Antona, Mazzitelli, & Ritter 1989). Since the new overadiabatic gradients can be substantially different from the MLT values, this mechanism must also be restudied using the new model.

In conclusion, the new theory, especially with $\Lambda = z$, constitutes a significant departure from the original MLT.

3.8. Future Work: Modeling Turbulence

As we have already discussed in § 2.8, a treatment of stellar turbulent convection must include the effects of compress-

ibility. In fact, in stellar interiors, the value of c_s is finite, and yet all available models of convective turbulence adopt the considerable simplification that $c_s \to \infty$. To be specific, let us formally write the convective flux as

$$F_c = F_c(\{\Gamma\}\Lambda) , \qquad (64)$$

where by $\{\Gamma\}$ we mean the functional dependence of F_c on the convective efficiency Γ. A complete theory would yield

$$\{\Gamma\} = \{\Gamma\}(c_s, \ldots) , \quad \Lambda = \Lambda(c_s, \ldots) \qquad (65)$$

for arbitrary values of c_s. What we have today are models that give us

$$\{\Gamma\} = \{\Gamma\}(c_s = \infty, \ldots) , \quad \text{i.e., incompressible ,}$$
$$\Lambda = \Lambda(c_s \neq \infty) = \alpha c_s^2/\gamma g \equiv \alpha H_p , \qquad (66a)$$

or

$$\Lambda = z , \quad \text{i.e., compressible ,} \qquad (66b)$$

leading to an expression for F_c in which turbulence is treated as incompressible but some of the parameters (Λ and the temperature gradient) attempt to account for compressibility effects. The situation is not fully satisfactory.

What one must strive for is a model of fully compressible turbulent convection. At present, we possess the formalism (Hartke et al. 1988a) to carry out a consistent treatment, but until specific results become available, it is impossible to predict whether F_c will increase or decrease. This is due to the following reason. Using equation (12), we can formally write

$$F_c(c_s) \propto E(c_s)n_s(c_s) , \qquad (67)$$

where we have explicitly exhibited c_s to indicate that we would like a result valid for arbitrary values of c_s. Rewrite formula (67) as

$$F_c(c_s) = \mu_1 \mu_2 F_c(\infty) , \qquad (68)$$

where $F_c(\infty)$ is the flux computed in this paper and where

$$\mu_1 = E(c_s)/E(c_s = \infty) , \qquad (69a)$$

$$\mu_2 = n_s(c_s)/n_s(c_s = \infty) . \qquad (69b)$$

Since on physical grounds one expects $\mu_1 < 1$ but $\mu_2 > 1$, it is not possible at this stage to know whether compressibility will increase or decrease the convective flux. The result $\mu_2 > 1$ is based on the energy principle (the more compressible the system, the more unstable it is [Schmidt 1966; Newcomb 1983]; for a convective instability see Böhm 1963, Chitre & Gokhale 1973, and Fox 1985; for a Rayleigh-Taylor instability see Bernstein & Book 1983). The reason why μ_1 is expected to be less than unity is as follows. The presence of compressibility means that *not* all the energy input into the fluid is going to generate turbulence: part of it will be used to excite compressible modes, e.g., sound waves, and so the resulting eddy energy spectrum will be reduced in magnitude. Mathematically, compressibility effects lead to a considerable complication of the equations, since there are now two spectral functions, the transverse one, $E_T(k)$, and the longitudinal one, $E_L(k)$. While only the first is needed to compute the convective flux, the two are coupled by nonlinear differential equations which must be solved simultaneously (Hartke et al. 1988a). Work in this direction is in progress.

4. CONCLUSIONS

In the first decades of this century, the mixing-length theory (MLT) was widely and rather successfully applied to engineer-ing flows by the schools of Prandtl and von Kármán, among others. It seems reasonable to speculate that the success and simplicity of the MLT might have been a strong incentive to adopt it to study turbulent convection in stars. The expectation has been amply rewarded, for the MLT has proved to be a very valuable tool. Regrettably, however, repeated attempts to improve the limitations inherent in the original MLT model have not succeeded, and today the MLT is still used in essentially its original form. In the terminology of Gough & Weiss (1976), the addition of "salt and pepper" to the original version of the MLT have not proved sufficient: new flavors must be added. We have identified the following two:

1. A turbulent viscous flow can reasonably be approximated by a one-mode, one-eddy, one–length scale model such as the MLT, since in fact the width of the turbulent spectrum of eddies is inversely proportional to viscosity (eq. [28]). Stellar interiors are, on the other hand, nearly inviscid, and the wide range of eddies that characterize them cannot be fully represented by a one-eddy model, like the MLT (Figs. 1–4). This point was also emphasized by Marcus, Press, & Teukolsky (1983). In adopting the MLT, one is bound to underestimate the flux (eq. [31]). Our first task was therefore to abandon the MLT one-mode approach, use two modern theories of turbulence, and compute the entire spectrum of eddies. This naturally leads to a larger flux (eq. [32]), in agreement with other authors (Chan & Sofia 1989; Cabot et al. 1990).

2. To account for compressibility effects, the MLT adopts the expression $\Lambda = \alpha H_p$. The ensuing values of α are usually larger than unity, implying a logical inconsistency with the premises of the model. We do not yet have a model for compressible turbulence, and so we must also rely on some expression for Λ derived from outside the model itself. When we adopt $\Lambda = \alpha H_p$, we find that, in contrast to the MLT, our α turns out to be less than unity, which is a welcome feature. However, we also present arguments to suggest that, in contrast to mechanically driven turbulence—which is usually a local, small-scale phenomenon, so that Λ cannot depend on the global variable z—thermally driven turbulence is not a local phenomenon. Furthermore, since in the absence of ν and χ (high convective efficiency) one cannot form a unit of length with the variables of the problem, the only remaining choice is $\Lambda = \Lambda(z)$, of which $\Lambda = z$ is the simplest form.

The new model was included in an evolutionary code, and representative evolutionary tracks were calculated. In a first treatment we used the new convective flux (eq. [32]) but retained the $\Lambda = \alpha H_p$ model. The results are similar to those of the MLT model but require $\alpha < 1$, thus easing some of the inconsistencies that the MLT has with $\alpha > 1$. A detailed study with the parameter-free $\Lambda = z$ formula was also made, and the results are promising. The latter formula did not give acceptable results when used in the MLT.

The main astrophysical result is that, with the new theory, the Sun has been fitted within $\sim 0.2\%$ accuracy without adjustable parameters. In addition, since the subatmospheric temperature and density profiles for the Sun are quite different from the MLT case, the helioseismological properties of the Sun are also expected to change. Work in this field is in progress (L. Paternò 1990, private communication).

The location in the H-R diagram of the evolutionary tracks of globular cluster stars is shifted toward lower surface temperatures. If confirmed by more extensive calculations, this would imply that the observed properties of globular clusters should be fitted by larger turnoff masses, and thus shorter ages, a result of possible cosmological significance.

Other astrophysical tests may be of interest. Perhaps the most immediate one, also in progress, is the detailed comparison of theoretical predictions with observational data pertaining to the lower main sequence, where the MLT predicts values of T_{eff} definitively larger than the observed values, while the new theory yields lower T_{eff} and thus in the right direction. The larger fluxes predicted by the new theory imply lower convective velocities, at least far from the peak of overadiabaticity very close to the surface of the star. This implies that convective overshooting will be reduced with respect to the MLT case.

The conceptual improvements with respect to the MLT, the lack of adjustable parameters, the quantitative fit to the data we have analyzed, as well as the qualitative indications that the model may solve other problems, seem to augur well for the future of the new model.

APPENDIX A

THE DIA MODEL OF TURBULENCE

The direct interaction approximation (DIA; Kraichnan 1964; Leslie 1973) is the most complete theory of turbulence, since it constitutes the most deterministic derivation of the equation for $E(k)$ from the full Navier-Stokes equations presently available. Introducing the notation

$$E(k) = 4\pi k^2 Q(k, 0) , \tag{A1}$$

the equation satisfied by $Q(k, \tau)$ is given by

$$\left[\frac{\partial}{\partial t} - n_s(k)\right] Q(k, t - s) = 2\pi \iint_\Delta kpq\, b(k, q, p) dp\, dq \left[\int_{-\infty}^{s} ds' G(k, s - s') Q(q, t - s') Q(p, t - s')\right.$$
$$\left. - \int_{-\infty}^{t} ds' G(q, t - s') Q(p, t - s') Q(k, s - s')\right]. \tag{A2}$$

The greater complexity of the equation for $E(k)$ within the DIA is due to the fact that while the triple correlation function θ of the EDQNM model must be prescribed from outside the model, within the DIA all the functions are prescribed self-consistently from within the theory. The physical analog of the function θ is the Green function (or infinitesimal response function) $G(k, \tau)$ which is obtained by solving the equation

$$\left[\frac{\partial}{\partial t} - n_s(k)\right] G(k, t - s) = -2\pi \iint_\Delta kqp\, b(k, q, p) dq\, dp \int_s^t ds' G(q, t - s') Q(p, t - s') G(k, s' - s) + \delta(t - s) . \tag{A3}$$

The function b is defined as $b(k, q, p) = (q/k)(xy + z^3)$, with the rest of the notation identical to that introduced in the main text.

Needless to say, the DIA equations are far more complex to solve than the EDQNM model. However, since we had coded them to study laboratory thermal convection (Hartke, Canuto, & Dannevik 1988b), we employed the same code to study the case of interest here. Because of the large demand in computer time, we did not solve them for all the cases of interest but only for few selected cases in order to compare them with the EDQNM results. In all cases of interest, the bulk properties of the two models (kinetic energy, convective flux, etc.) did not differ significantly from the EDQNM values.

APPENDIX B

THE EDQNM MODEL

To appreciate the physics contained in $T(k)$ (eq. [21]), we first note that the interactions contributing to $T(k, t)$ are of two kinds: *local* and *nonlocal*. In the first case the wavenumbers k, p, and q are of the same order, while in the second case one of the wavenumbers is either much smaller or larger than the other two. In what follows, we shall give the expressions for the nonlocal interactions, since they allow an interesting physical interpretation. They are defined by

$$k \ll p \approx q , \tag{B1}$$

$$q \ll k \approx p . \tag{B2}$$

In the first case $T(k)$ is expanded in powers of $k/p \ll 1$, while in the second case the expansion is in powers of $q/k \ll 1$. These expansions correspond to different physical processes. In practice, one performs the expansion not in $T(k)$ but in the function $\Pi(k)$

which is obtained after integrating (20) from 0 to k. We have [$y(k)$ is the mean squared vorticity]

$$-\frac{\partial}{\partial t}\int_0^k E(q, t)dq + \epsilon(k, t) = 2vy(k, t) + \Pi(k, t) , \tag{B3}$$

$$T(k, t) \equiv -\frac{\partial}{\partial k}\Pi(k, t) , \qquad y(k) \equiv \int_0^k p^2 E(p)dp , \tag{B4}$$

$$\epsilon(k) \equiv 2\int_0^k [n_s(p) + vp^2]E(p)dp . \tag{B5}$$

The physical interpretation of equation (B3) is best seen in the stationary case: $\epsilon(k)$ represents the input of energy (from the instability n_s) into the wavenumber region from 0 to k; this energy is partly dissipated into heat by kinematic viscosity v and partly transferred to all the remaining eddies by the nonlinear interactions represented by $\Pi(k)$. The nonlinear terms are neither a source nor a sink of energy; they redistribute the available energy among eddies of different sizes, and thus they do not contribute to the total balance of energy. If we extend the wavenumber k to ∞, we obtain ϵ:

$$\epsilon = 2v\int_0^\infty p^2 E(p)dp , \tag{B6}$$

which means that all the energy input is dissipated into heat by viscous forces.

Performing the expansions (B1) and (B2), we derive (NL = nonlocal)

$$\Pi \rightarrow \Pi_{NL} = \Pi_a + \Pi_b , \tag{B7}$$

$$\Pi_a = \Pi_a^{(1)} + \Pi_a^{(2)} , \tag{B8}$$

and similarly for Π_b. The results are

$$\Pi_a^{(1)} = 2y(k, t)v_t(k, t) , \tag{B9}$$

$$v_t(k, t) = \tfrac{1}{15}\int_k^\infty \theta(p, t)[5E(p, t) + pE'(p, t)]dp , \tag{B10}$$

$$\Pi_a^{(2)} = -\frac{14}{15}\int_0^k q^4 dq \int_k^\infty \left[\frac{E(p, t)}{p}\right]^2 \theta(p, t)dp$$

$$= -B(k)Z(k) , \tag{B11}$$

where $B(k)$ and $Z(k)$ represent the first and second integrals and $E' = dE(p)/dp$. To clarify the physical meaning of the new term $\Pi_a^{(2)}$, substitute equation (B7) in equation (B3), take the derivative with respect to k, and consider the stationary state. Grouping terms gives a balance of sources (left side) and sinks (right side), with $v'(k) < 0$,

$$n_s(k) - v_t'(k)\frac{y(k)}{E(k)} + \frac{1}{2}k^4\frac{Z(k)}{E(k)} = v_t(k)k^2 + \frac{1}{2}k^{-2}\theta(k)B(k)E(k) . \tag{B12}$$

The various terms may be interpreted as follows (Fig. 13). The first term on the left represents the contribution from the source to the group of eddies around the wavenumber k. The second term on the left represents the contribution of all the eddies with wavenumbers in the interval $[0, k]$. The third term on the left represents the contribution from all the eddies with wavenumbers in the interval (k, ∞) and is, therefore, a backscatter term. The first term on the right represents the loss of energy to the eddies with wavenumbers in the interval (k, ∞) via a turbulent viscosity. Finally, the second term on the right represents a loss of energy to the eddies with wavenumbers in the interval $[0, k]$.
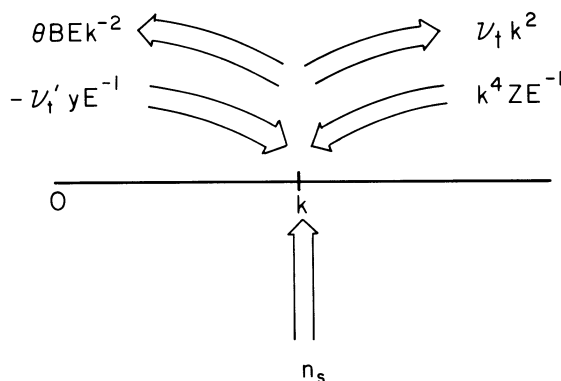

FIG. 13.—Schematic representation of the energy balance (eq. [B12]), showing the various sources and sinks at wavenumber k.

Next, consider the process given by equation (B2). The expansion of $\Pi(k, t)$ in powers of q/k gives

$$\Pi_b^{(1)} = \tfrac{2}{15}\, \theta(k,\, t)y(k,\, t)[kE(k,\, t) - k^2 E'(k,\, t)] \, , \tag{B13}$$

$$\Pi_b^{(2)} = \tfrac{2}{75}\, k^4\theta(k,\, t)E^2(k,\, t) \, . \tag{B14}$$

While $\Pi_b^{(2)}$ does not have a direct physical interpretation (it may be shown to be a higher order term that contributes little to the energy spectrum), $\Pi_b^{(1)}$ (an expression similar to one originally proposed by Obukhov) shows that the energy transfer across a wavenumber k is analogous to the energy transfer from the mean flow to turbulence via Reynolds stresses: eddies with wavenumbers greater than k provide the Reynolds stress that Obukhov wrote as the integral of $E(k)$ from k to ∞, while the mean rate of strain was taken to be $y^{1/2}(k)$. Since it was later noted that this expression gave unphysical results, a new form, known as the modified Obukhov transfer, was proposed, i.e., $kE(k)y^{1/2}(k)$.

REFERENCES

Batchelor, G. K. 1953. Theory of Homogeneous Turbulence (Cambridge: Cambridge Univ. Press)
Bernstein, I. B. & Book, D. L. 1983, Phys. Fluids, 26, 453
Biermann, L. 1948, Zs Ap., 25, 135
Böhm, K. H. 1963, ApJ, 137, 881
Böhm-Vitense, E. 1958, Zs. Ap., 46, 108
Bressan, A. G., Bertelli, G., & Chiosi, C. 1986, Mem. Soc. Astr. Italiana, 57, 411
Burrows, A., Hubbard, W. B., & Lunine, J. I. 1989, ApJ, 345, 939
Cabot, W., Hubickyj, O., Pollack, J. B., Cassen, P., & Canuto, V. M. 1990, Geophys. Ap. Fluid Dyn., 53, 1
Canuto, V. M., & Goldman, I. 1985, Phys. Rev. Letters, 54, 430
Canuto, V. M., & Hartke, G. J. 1986, A&A, 168, 89
Caputo, F., Castellani, V., Chieffi, A., Pulone, L., & Tornambè, A. 1989, ApJ, 340, 241
Chan, K. L., & Sofia, S. 1989, ApJ, 336, 1022
Chan, K. L., Sofia, S., & Wolff, C. L. 1982, ApJ, 263, 935
Chandrasekhar, S. 1961, Hydrodynamic and Hydromagnetic Stability (New York: Oxford Univ. Press)
Chimonas, G. 1970, J. Fluid Mech., 43, 833
Chitre, S. M., & Gokhale, M. H. 1973, Solar Phys., 30, 309
Cloutman, L. D. 1979, ApJ, 227, 614
Cox, A. N., & Stewart, J. J. 1970, ApJS, 19, 243
Cox, J. P., & Giuli, R. T. 1968, Principles of Stellar Structure (New York: Gordon & Breach) (CG68)
D'Antona, F., Mazzitelli, I., & Ritter, H. 1989, A&A, 225, 391
Dziembowski, W. A., Paternò, L., & Ventura, R. 1988, A&A, 200, 213
Einaudi, F. 1980, in Atmospheric Boundary Layer Physics (New York: Elsevier), 77
Fox, P. A. 1985, Ph.D. thesis, Monash Univ.
Gilman, P. A., & Glatzmeier, G. A. 1981, ApJS, 45, 335
Gilman, P. A., & Miller, J. 1986, ApJS, 61, 585
Gough, D. O., & Weiss, N. O. 1976, MNRAS, 176, 589
Hartke, G. J., Canuto, V. M., & Alonso, C. 1988a, Phys. Fluids, 31, 1034
Hartke, G. J., Canuto, V. M., & Dannevik, W. P. 1988b, Phys. Fluids, 31, 256
Hossain, M. H., & Mullan, D. J. 1990, ApJ, 354, L33
Huebner, W. F., Merts, A. L., Magee, N. H. Jr., & Argo, M. F. 1977, Astrophysical Opacity Library, UC-34b
Hurlburt, N. E., Toomre, J., & Massaguer, J. M. 1984, ApJ, 282, 557
Kaimal, J. C., Wyngaard, J. C., Izumi, Y., & Coté, O. R. 1972, Quart. J. Roy. Meteorol. Soc., 98, 536
Kraichnan, R. H. 1964, Phys. Fluids, 7, 1030
———. 1987, Phys. Fluids, 30, 1583

Landau, L. D., & Lifshitz, E. M. 1987, Fluid Mechanics (2d ed.; New York: Pergamon)
Langer, N. 1986, A&A, 164, 45
Lattanzio, J. C. 1989, ApJ, 344, L25
Lesieur, M. 1987, Turbulence in Fluids (Dordrecht: Nijhoff)
Leslie, D. C. 1973, Developments in the Theory of Turbulence (Oxford: Clarendon)
Maeder, A., & Meynet, G. 1989, A&A, 210, 155
Marcus, P. S., Press, W. H., & Teukolsky, S. A. 1983, ApJ, 267, 795
Massaguer, J. M. 1990, in Inside the Sun, ed. G. Berthomieu & M. Cribier (Dordrecht: Kluwer), 101
Massaguer, J. M., & Zahn, J.-P. 1980, A&A, 8, 315
Mazzitelli, I. 1979, ApJ, 79, 251
———. 1989a, ApJ, 340, 249
———. 1989b, in IAU Colloquium 114, White Dwarfs, ed. G. Wegner (New York: Springer-Verlag), 29
Monin, A. S., & Obukhov, A. M. 1954, USSR Acad. Sci. Geophys. Inst., No. 24
Monin, A. S., & Yaglom, A. M. 1975, Statistical Fluid Mechanics (Cambridge: MIT Press)
Newcomb, W. A. 1983, Phys. Fluids, 26, 3246
Orszag, S. A. 1977, in Fluid Dynamics, Les Houches Summer School of Theoretical Physics, ed. R. Balian & J. L. Peube (New York: Gordon & Breach), 237
Pederson, B. B., VandenBerg, D. A., & Irwin, A. W. 1990, ApJ, 352, 279
Prandtl, L. 1925, Zs. Angew. Math. Mech., 5 (No. 2), 136
Priestley, C. H. B. 1959, Turbulent Transfer in the Lower Atmosphere (Chicago: Univ. Chicago Press)
Rayleigh, Lord. 1916, Phil. Mag., 32, 529
Renzini, A. 1987, A&A, 188, 49
Schmidt, G. 1966, Physics of High Temperature Plasmas (New York: Academic), 135
Spiegel, E. A., & Moore, R. L. 1964, ApJ, 139, 48
Spruit, H. C., Nordlund, A., & Title, A. M. 1990, ARA&A, Vol. 29, 263
Stein, R. F., & Nordlund, A. 1989, ApJ, 342, L95
Tassoul, M., Fontaine, G., & Winget, D. E. 1990, ApJS, 72, 335
VandenBerg, D. A., & Bell, R. A. 1985, ApJS, 58, 561
Vitense, E. 1953, Zs. Ap., 32, 135
von Kármán, T. H. 1930, in Proc. Third Internat. Conf. Appl. Math. (Stockholm), Part 1, p. 85
Yakhot, V., & Orszag, S. A. 1986, J. Sci. Computing, 1, 1
Yamaguchi, S. 1963, PASJ, 15, 412